Recognition and Reaction of Metallointercalators with DNA

Kathryn E. Erkkila, Duncan T. Odom, and Jacqueline K. Barton*

Division of Chemistry, California Institute of Technology Pasadena, California 91125

Received May 17, 1999 (Revised Manuscript Received July 5, 1999)

Contents

1. Introduction

The design of small complexes that bind and react at specific sequences of DNA becomes important as we begin to delineate, on a molecular level, how genetic information is expressed. A more complete understanding of how to target DNA sites with specificity will lead not only to novel chemotherapeutics but also to a greatly expanded ability for chemists to probe DNA and to develop highly sensitive diagnostic agents.

Transition-metal complexes are being used at the forefront of many of these efforts. Stable, inert, and water-soluble complexes containing spectroscopically active metal centers are extremely valuable as probes of biological systems. As both spectroscopic tags and functional models for the active centers of proteins, metal complexes have helped elucidate the mechanisms by which metalloproteins function. More recently, such metal complexes have been applied to probe both structural and functional aspects of nucleic acid chemistry.

Here we review developments in the area of metallointercalators that bind and react with DNA. Intercalators are small molecules that contain a planar aromatic heterocyclic functionality which can insert and stack between the base pairs of double-helical DNA.[1] Lippard and co-workers first established that square planar platinum(II) complexes containing an aromatic heterocyclic ligand could bind to DNA by intercalation.[2] In our laboratory, metallointercalation was extended to three dimensions using octahedral complexes. The application of octahedral metallointercalators has permitted the targeting of specific DNA sites by matching the shape, symmetry, and functionalities of the metal complex to that of the DNA target. Moreover, by taking advantage of the photophysical, photochemical, and redox properties of metallointercalators, sensitive spectroscopic and reactive probes of DNA have been developed. Our review of this rich chemistry of metallointercalators is not intended to be exhaustive. Instead, it is intended to serve as a report that highlights varied characteristics of metallointercalators and ones that make metallointercalators powerful agents for probing and targeting nucleic acids.

2. Recognition of DNA by Metallointercalators

2.1. Background—Early Metal Complexes

The first experiments describing the interaction of coordinatively saturated octahedral transition-metal complexes with DNA involved the use of complexes that had been chemically well characterized in many other contexts. These early studies focused on the

* To whom correspondence should be addressed.

10.1021/cr9804341 CCC: $35.00
Published on Web 08/03/1999

Kathryn E. Erkkila, of Albuquerque, NM, graduated with her A.B. in Chemistry from Bryn Mawr College in 1992. After a year at Sandia National Laboratories as an Associated Western Universities Fellow, she joined Professor Jacqueline Barton's laboratory at California Institute of Technology in 1993. Her thesis project focuses on photochemical and structural characterizations of phi complexes of rhodium(III) and iridium(III) bound to DNA.

Duncan Odom graduated with his B.A. from New College in Sarsota, FL, in 1994. He is presently a student in the laboratories of Professor Jacqueline Barton at the California Institute of Technology. His doctoral research focuses on the interactions of site-specific metal complexes as potential therapeutics and on long-range electron transfer through unusual nucleotide structures.

binding of tris(phenanthroline) complexes of zinc, cobalt, and ruthenium to DNA[3−11] (Figure 1). On the basis of photophysical and NMR studies, it was proposed that the cationic tris(phenanthroline) complexes bound to DNA through three noncovalent modes: (i) electrostatically; (ii) binding hydrophobically against the minor groove; and (iii) partial intercalation of one of the phenanthroline ligands into the DNA base stack from the major groove side. Early experiments indicated a preference for the right-handed Δ-isomers upon intercalation into right-handed DNA, while a small preference for the Λ-isomers could be observed for binding in a complementary fashion against the right-handed groove.[10] While the binding interactions of these complexes have been debated,[12−14] their enantiomeric preferences have been seen quite consistently in derivative complexes prepared since those early experiments, as will be evident throughout this review. Chiral discrimination of this type clearly depends on matching the symmetry of the metal complex with that of the double helix.

Dr. Jacqueline K. Barton is the Arthur and Marian Hanisch Memorial Professor of Chemistry at the California Institute of Technology. Barton was awarded her B.A. degree summa cum laude at Barnard College in 1974 and went on to receive her Ph.D. in Inorganic Chemistry at Columbia University in 1979 in the laboratory of S. J. Lippard. After a post-doctoral fellowship at Bell Laboratories and Yale University, she joined the faculty at Hunter College, City University of New York. In 1983, she returned to Columbia University, becoming Associate Professor of chemistry and biological sciences in 1985 and Professor in 1986. In the fall of 1989, she joined the faculty at Caltech. Professor Barton has pioneered the application of transition-metal complexes as tools to probe recognition and reactions of double-helical DNA. Using chiral coordination complexes, she has designed octahedral metal complexes which recognize nucleic acid sites with high affinities and specificities. With these transition-metal probes, she has also carried out critical studies to elucidate electron-transfer chemistry mediated by the DNA base pair stack. Barton is the author of more than 150 publications and has received numerous awards for her work, including, from the ACS, the Award in Pure Chemistry, the Eli Lilly Award in Biological Chemistry, the Garvan Medal, and, most recently, the Nichols Medal.

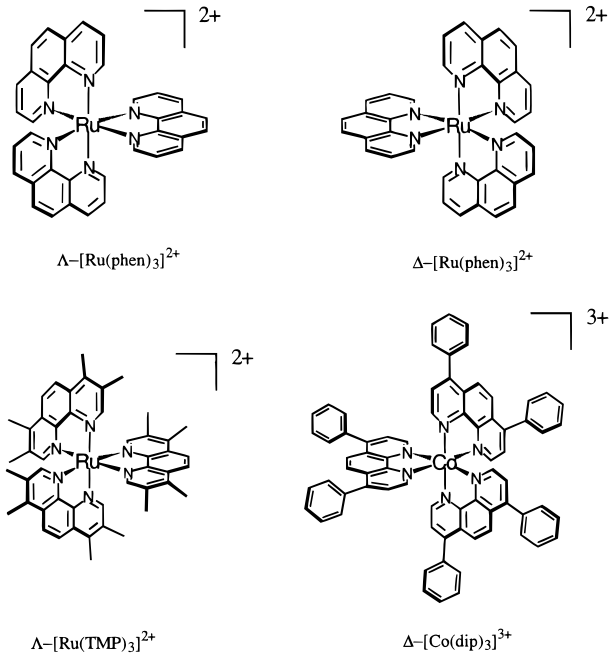

Figure 1. Early octahedral DNA probes.

Studies with these simple complexes provided a basis for conceptualizing how octahedral complexes might interact noncovalently with DNA and for exploring how the properties of the metal complexes, most notably their photophysical and redox characteristics, might be utilized in developing novel probes for DNA. Nonetheless, the binding affinities of these complexes for DNA were unimpressive, and the

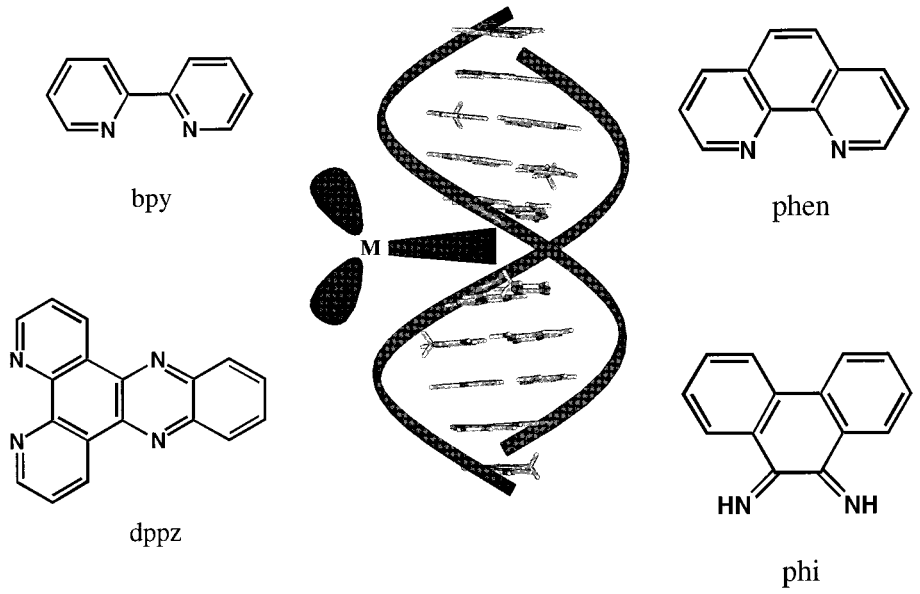

Figure 2. Ancillary and intercalating ligands, and (center) an illustration of an intercalating complex oriented with respect to the DNA double helix.

mixture of binding modes, depending upon sequence, salt, and temperature, became problematic. In order for octahedral metallointercalators to become useful in biological applications and assays and, indeed, for intercalation to dominate as the mode of interaction, the intercalative binding affinities had to be significantly increased.

2.2. Increasing DNA Affinity and Discrimination by Intercalation

2.2.1. Intercalation as a Platform for Binding

Increasing the surface area for intercalative stacking by a complex leads to a substantial increase in intercalative binding affinity. As a result, metallointercalators which contain an extended aromatic heterocyclic ligand can provide immensely powerful tools to probe nucleic acids.[15−18] By inserting and stacking between the base pairs, octahedral complexes containing the 9,10-phenanthrenequinone diimine (phi) or dipyrido[3,2-*a*:2′,3′-*c*]phenazine (dppz) ligand provided predictable, stable anchors in the major groove with a known orientation of all the functionalities on the metal complex established with respect to the DNA duplex (Figure 2). In combination with the stable ligand architecture of late transition metal complexes, this type of anchor can be exploited to generate chiral discrimination and sequence specificity comparable to that of DNA binding proteins.

2.2.2. Metal Complexes of Dipyridophenazine and Derivatives

Bipyridyl and phenanthroline complexes of ruthenium containing the dppz ligand intercalate relatively nonspecifically into B-form DNA with a slight preference for AT-rich regions.[19] The dppz complexes, with their expansive aromatic surface area, show extremely high affinity for DNA, with binding constants $>10^6$ M^{-1}.[20] Analogous ruthenium(II) complexes, with 1,4,5,8-tetraazaphenanthrene (TAP), 1,4,5,8,9,12-hexaazatriphenylene (HAT), and

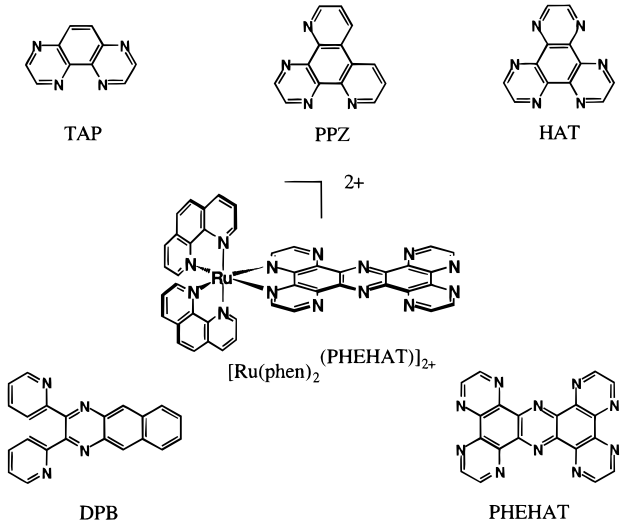

Figure 3. dppz-like intercalating ligands, and a PHEHAT complex of Ru(II).

1,10-phenanthrolino[5,6-*b*]1,4,5,8,9,12-hexaazatriphenylene (PHEHAT), also interact with DNA and, like dppz complexes, show changes in photophysical properties upon binding to the DNA duplex.[21] Bimetallic complexes bridged by the 2,3-bis(2-pyridyl)-benzo[*g*]quinoxaline (dpb) ligand have also been shown to bind to DNA by intercalation[22] (Figure 3).

2.2.2.1. Metal Complexes as Molecular Light Switches. $[Ru(bpy)_2(dppz)]^{2+}$ and related derivative complexes in organic solutions show solvatochromic luminescence to varying degrees. However, in aqueous solution, these complexes do not luminesce due to the ability of water to deactivate the excited state through hydrogen bonding with the intercalating ligands.[20,23,24] Interestingly, upon introduction of B-form, double-helical DNA to an aqueous solution of any of these metal complexes, photoluminescence is observed, reflecting the shielding of the intercalating ligand from bulk solvent. This is akin to introducing the complex into a local organic solvent that shields the ring nitrogens on the intercalating ligand from

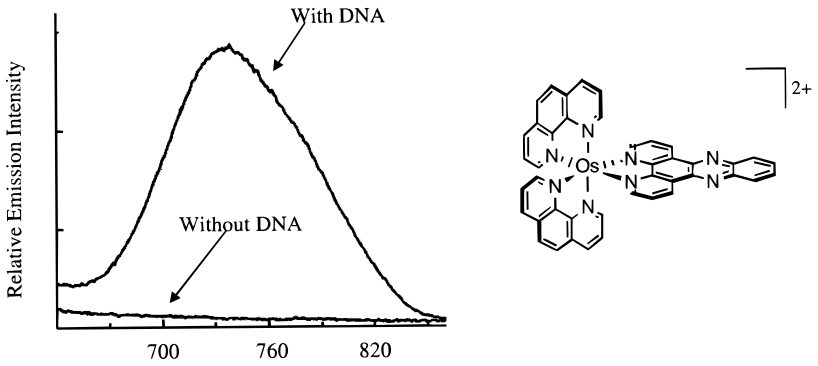

Figure 4. $[Os(phen)_2dppz]^{2+}$ and the "light switch" effect on complex luminescence. In water the luminescence is quenched (lower spectrum), but in DNA, the intercalated ligand is protected from solvent quenching, giving rise to observable luminescence (upper spectrum).

protonation. It is this effect that has been extensively characterized and described as the "molecular light switch". In the case of $[Ru(phen)_2dppz]^{2+}$ bound to DNA, the excited-state lifetime is approximately 200 ns, whereas free in aqueous solution, the lifetime of the excited state is only 200 ps.[24] This light switch effect is quite remarkable and provides the basis for a valuable photophysical probe of nucleic acids.

$[Ru(phen)_2PHEHAT]^{2+}$ was also found to be a light switch, although it displayed a weaker luminescence when bound to calf thymus DNA than did $[Ru(phen)_2dppz]^{2+}$.[25] $[Ru(phen)_2HAT]^{2+}$, unlike $[Ru(phen)_2PHEHAT]^{2+}$ and $[Ru(phen)_2dppz]^{2+}$, luminesces in aqueous solution, but this luminescence is only slightly enhanced in the presence of DNA.[26] Some of these derivatives, in fact, show decreased luminescence bound to GC-rich DNAs as a result of electron-transfer quenching. The photophysics and photochemistry of both osmium(II) and ruthenium(II) complexes of HAT, PHEHAT, and several other related polypyridyl ligands in the presence of DNA and single nucleotides has been the subject of a recent review.[21]

Luminescent characteristics of these complexes bound to DNA can also be used to illustrate the chiral discrimination associated with binding to the right-handed helix. Although the discrimination in binding is not high with phenanthrolines as ancillary ligands, it is interesting that in binding to calf thymus DNA at a loading of 1:25 base pairs, the excited-state lifetimes of Δ-$[Ru(phen)_2dppz]^{2+}$ and Λ-$[Ru(phen)_2dppz]^{2+}$ are $t_1 = 160$ ns, $t_2 = 850$ ns and $t_1 = 40$ ns, $t_2 = 150$ ns, respectively.[27] It is the right-handed isomer that is bound more deeply within the right-handed helix, yielding longer excited-state lifetimes. Analogous results were seen in the chiral discrimination of DNA by Δ- and Λ-isomers of $[Ru(bpy)_2L]^{2+}$ complexes where L = the intercalating ligand ppz (ppz = 4,7-phenanthrolino-[5,6-*b*]-pyrazine).[28]

2.2.2.2. Variations in the Complex. The systematic introduction of variations onto the terminal aromatic ring of the dppz ligand of $[Ru(phen)_2dppz]^{2+}$ has been carried out to provide a host of luminescent probes of DNA.[29] The complexes containing modified dppz ligands are not as sensitive to aqueous quenching of luminescence as the parent compound, and, thus cannot be accurately described as "light switches". The modified complexes, however, show a wide variety of spectroscopic profiles.

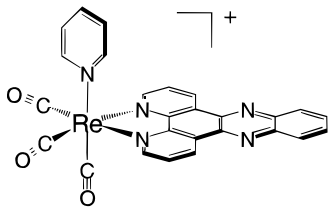

Figure 5. $[Re(CO)_3(py)dppz]^{+}$.

Replacement of the ruthenium with osmium as the central metal ion causes the luminescence observed for Ru(II) with a maximum of 620 nm to red-shift to 738 nm[30] (Figure 4). Hence, $[Os(phen)_2dppz]^{2+}$ can act as a red-emitting luminescent reporter for the presence of DNA. Recently, experiments varying the dppz ligand functionality similarly to those performed for $[Ru(phen)_2dppz]^{2+}$ have been carried out for osmium.[31] $[Co(phen)_2dppz]^{3+}$ has also been constructed. This analogue binds to DNA with high affinity and is able to cleave DNA when photoirradiated.[32] The Ni(II) complex, $[Ni(phen)_2dppz]^{2+}$, has also been prepared and may prove to be useful in carrying out paramagnetic NMR experiments.[32]

Finally, rhenium has been used in the construction of luminescent metallointercalators; $[Re(CO)_3(py)dppz]^{+}$ has been shown to have the same light switch capabilities as dppz complexes of Ru(II)[33] (Figure 5). This complex was also found to bind tightly to calf-thymus DNA and, when irradiated, to promote strand scission on pBR322.[34]

2.2.2.3. Intercalation through the Major Groove. Given the potential utility of the dppz complexes and their derivatives, it becomes important to develop a detailed structural understanding of how these complexes interact with the helix. Both photophysical studies and linear dichroism studies provided support for intercalation.[20,29,35−38] Additionally, consistent with the early intercalative models,[10] as mentioned above, it was observed that the Δ-isomer showed greater luminescence bound to right-handed DNA than did the Λ-isomer. Calorimetry studies established the high affinity of both complexes in binding the DNA duplex.[39]

The luminescent characteristics of the dppz complexes bound to DNA in general showed a biexponential decay in emission, with the percentages of the two components varying as a function of DNA sequence. On this basis, two general orientations for

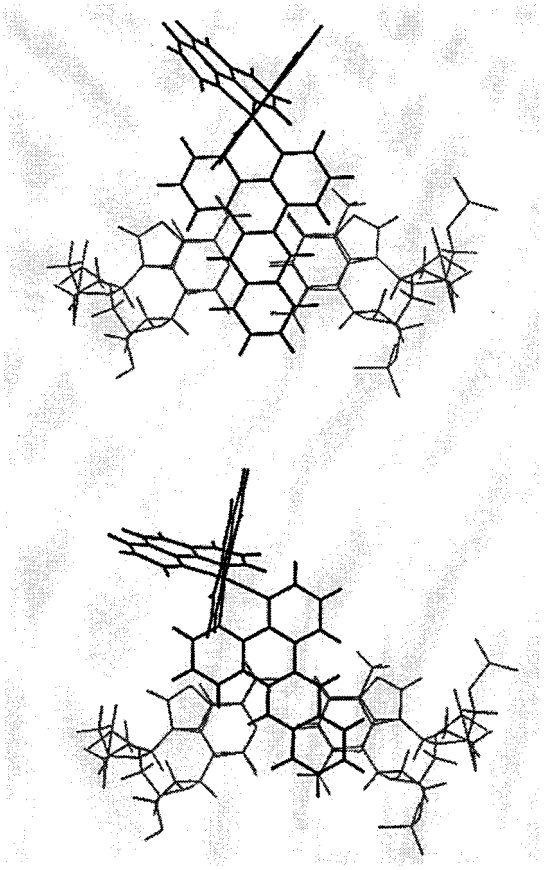

Figure 6. Depiction of two proposed binding modes of [Ru(phen)$_2$dppz]$^{2+}$ to DNA. The stacking of a dppz complex on the DNA base pair is shown looking down the helix axis. The head-on mode (upper) is illustrated with both phenazine nitrogens fully protected within DNA stack. The side-on mode (lower) is shown with one partially exposed phenazine nitrogen.

intercalation of the complexes into DNA were proposed[29,35] (Figure 6). The longer-lived component was assigned to a "head-on" binding mode; in this mode, both nitrogens of the phenazine ligand are equally protected by intercalation from solvent quenching. Similarly, the shorter component, more easily quenched, was assigned to a "side-on" binding mode, where the dppz ligand was stacked at an angle with respect to the helical dyad axis.

While an intercalative mode of interaction was clear, some controversy surrounded the groove position of the ruthenium intercalators on the DNA helix. Early NMR experiments, including intermolecular NOE's to major groove protons, indicated that the complex binds through the major groove.[40] However, other researchers reported photophysical studies showing that [Ru(bpy)$_2$(dppz)]$^{2+}$ did not significantly decrease its luminescence when bound to T4-DNA, which is heavily glucosylated in the major groove by cytosine derivatization.[36] This observation, together with more indirect lines of evidence, seemed to suggest that the steric accessibility of the major groove was unimportant for [Ru(bpy)$_2$(dppz)]$^{2+}$ binding and, hence, that [Ru(bpy)$_2$(dppz)]$^{2+}$ might instead intercalate via the minor groove.

To explore this issue more fully, direct competition experiments[19] were performed with the minor groove binding reagent distamycin and the well-characterized, major groove binding molecule Δ-α-[Rh[(R,R)-Me$_2$trien]phi]$^{3+}$ ((R,R)-Me$_2$trien = 2*R*,9*R*-diamino-4,7-diazadecane) for which there is both a high-resolution NMR structure[41] and recently a full crystal structure[42] of the metal complex intercalated into a DNA duplex from the major groove (vide infra). These experiments showed that Δ−α-[Rh[(R,R)-Me$_2$trien]-phi]$^{3+}$ directly displaced Δ-[Ru(phen)$_2$dppz]$^{2+}$ from the DNA helix. In contrast, distamycin competition experiments showed that the luminescence of the metal complex, bound to various sequences of DNA, was unaffected by the presence of excess minor groove binder. These results were therefore consistent with the DNA helix simultaneously accommodating [Ru(phen)$_2$dppz]$^{2+}$ and distamycin, a minor groove binder. Additionally, [Ru(phen)$_2$dppz]$^{2+}$ was shown to have a slight, but significant, preference for poly-d(AT) over poly-d(GC), which resolved the apparent contradiction of major groove intercalation into T4-modified DNA. [Ru(phen)$_2$dppz]$^{2+}$, being preferentially intercalated into AT regions within the major groove, would not be seriously disrupted by major groove glucosylation of cytosines.

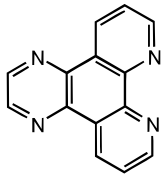

Figure 7. The dpq ligand.

NMR studies, which extended the original report of major groove intercalation based on selective deuteration of the dppz ligand, also confirmed the correlation of the biexponential decay of luminescence with the presence of two populations of intercalation geometries.[43] Two major orientations were proposed for the intercalation of this metal complex into B-form DNA. Centering the dppz ligand symmetrically along the dyad axis of DNA affords even shielding of the phenazine ligand, whereas the canted intercalation that maximizes base overlap greatly favors shielding primarily of only one-half of the dppz intercalator. The latter orientation provides very different chemical environments for the 4′ and 7′ dppz protons, which are indistinguishable in the absence of DNA. These two modes of binding could account for the biexponential decay of the dppz luminescence signal based on differential accessibility of the phenazine nitrogens to aqueous quenching in different binding orientations.[35]

2.2.2.4. Minor Groove Binding of [Ru(phen)$_2$-dpq]$^{2+}$. Removal of the terminal aromatic ring on the dppz ligand yields dipyrido[2,2-*d*:2′,3′-*f*]quinoxaline (dpq), a closely related analogue to dppz[44,45] (Figure 7). [Ru(phen)$_2$dpq]$^{2+}$ also intercalates into DNA, but NMR studies similar to those described above for [Ru(phen)$_2$dppz]$^{2+}$ have shown that [Ru(phen)$_2$dpq]$^{2+}$ binds from the minor groove side.[44−46] The binding affinity of the complex for DNA has not been determined nor is one isomer preferred over the other in binding. It is remarkable how apparently minor changes in the ligand architecture and electronic structure can lead to profound influences on binding geometries.

What, then, determines the groove access of the metallointercalators? Certainly it is not simply a steric consideration that governs the groove position of the intercalator. Indeed, a crystal structure of a square planar platinum intercalator bound within a dinucleotide duplex shows intercalation of the coordinated ligand from the major groove side.[47] In the coming years, it will be important to establish predictably those factors which govern groove position for the intercalator.

2.2.3. Porphyrin Intercalation into DNA

An additional large heterocyclic surface used for DNA intercalation is the porphyrin ring system. It has been long known that porphyrins bind to DNA, but the mode of binding has been debated.[48] Spectroscopic data indicate that porphyrins can bind to GC-rich sequences intercalatively, while in AT-rich regions they take on an external binding mode.[49] How such an intercalation can occur has been questioned, however, given the substantial size of the porphyrin ring versus that of the base pair. Free porphyrins and porphyrins bound to metals which do not take on axial ligands, such as Cu(II) and Ni(II), were suggested to intercalate most easily into DNA,[49−51] while metalated porphyrins which have axial ligands such as Co(II), Fe(II), Zn(II), and Mn(II) did not appear to intercalate.[50]

A far clearer understanding of how porphyrins interact with DNA emerged when the crystal structure of a copper porphyrin, [CuTMPPyP4] (copper(II) *meso*-tetra(*N*-methyl-4-pyridyl)porphyrin), bound to 5′-CGATCG-3′ was solved.[52] The most intriguing aspect of this crystal structure was that the porphyrin was seen to hemi-intercalate at the end of the DNA oligomer by displacing a cytosine from the terminal GC base pair. The orphan cytosine then base pairs with a guanine in a separate double helix so that there are no nonpaired extrahelical bases. Intercalation by a metal complex, in this view, represents a substantial perturbation of the DNA helix with base displacement being accompanied by binding (Figure 8). Indeed, in this instance, direct stacking of the porphyrin within the DNA helix does not seem to occur. While subsequent high-resolution views of Δ-α-[Rh[(R,R)Me_2trien]phi]$^{3+}$ bound to DNA gave a more classic picture of intercalation within a DNA helix,[42] this structure reminds us of the critical importance of continuing to establish a structural foundation for all new designs of metal complexes which bind DNA.

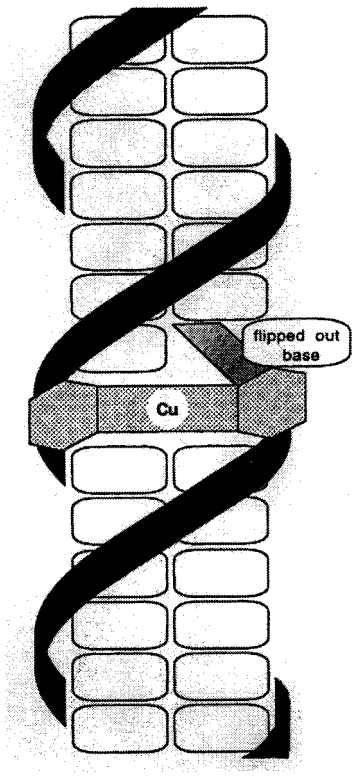

Figure 8. Schematic illustration of [CuTMPPy_4] porphyrin hemi-intercalating into DNA double helix, forcing cytosine into an extra-helical conformation. (Reprinted with permission from ref 52. Copyright 1996 American Chemical Society.)

2.3. DNA Recognition Based on Shape Selection

Due to their shape and polarity, different intercalating ligands stack with different orientations within the double helix and, as such, provide somewhat different strategies for the specific recognition of sites on DNA. Phenanthroline and bipyridine ligands are sterically compact, and metal complexes with these ligands have relatively shielded surfaces. This steric shielding prevents tris(phenanthroline) complexes from intercalating deeply into the B-form base stack and leads to its low binding affinities. Metal complexes containing a coordinated dppz ligand, in contrast, extend a heterocyclic ring system out from the central compact [Ru(bpy)$_3$]$^{2+}$ core and provide a substantial aromatic surface for intercalation in DNA. Because of the large expanse of the ligand, a family of orientations within the base stack appears to be available.

The 9,10-phenanthrenequinone diimine (phi) ligand provides different constraints and opportunities. When incorporated into an inert transition-metal complex, the phi ligand projects far from the metal center, due to the use of imines as coordinating chelators. Hence, like dppz, phi also presents an intercalating aromatic system that is removed from the metal center, yet the geometry of the phi ligand is such as to provide an expanse of aromatic structure across the base pair rather than along the dyad axis. In fact, the phi ligand was first designed in an attempt to match the positioning of aromatic rings with those of the base pairs.[53] The nonintercalating, ancillary ligands are brought into position against the DNA base pairs, and as a result, specific noncovalent interactions between the ancillary ligand functionalities and functionality in the DNA groove can be made.

The phi complexes also differ from the dppz complexes in terms of their photochemistry and, thus, in terms of their utilization. Phi complexes of both rhodium and ruthenium show no detectable photoinduced emission and, therefore, no photophysical signature to exploit.[54] Nonetheless, phi complexes of rhodium have a rich photochemistry. We have continually exploited the ability of phi complexes of rhodium(III) to cleave DNA at the site of intercalation

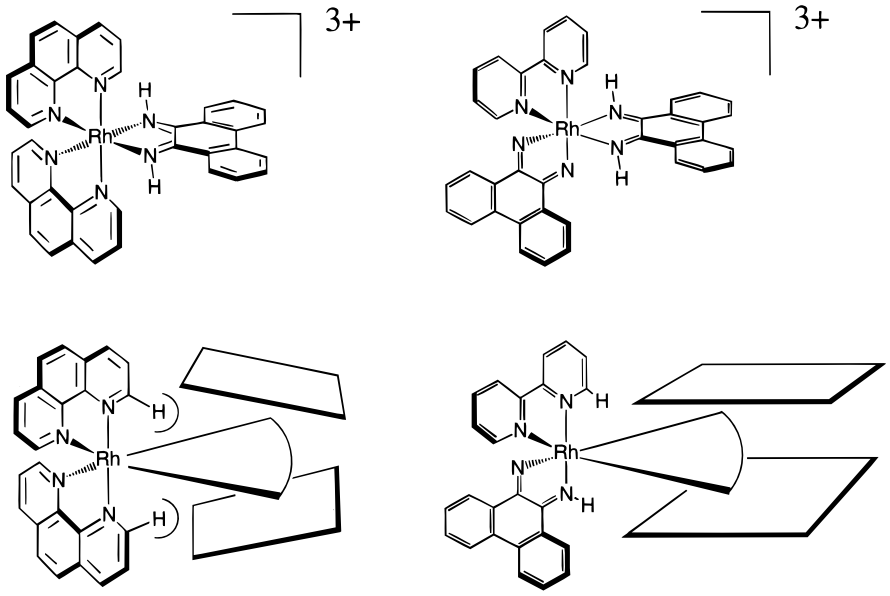

Figure 9. $[Rh(phen)_2phi]^{3+}$ (upper left) and $[Rh(phi)_2bpy]^{3+}$ (upper right) and illustration of steric interactions of $[Rh(phen)_2phi]^{3+}$ with propeller-twisted intercalation site (lower left) and $[Rh(phi)_2bpy]^{3+}$ with an ordinary intercalation site (lower right).

when irradiated with high-energy light (310−320 nm) (vide infra). This photochemical marking of sites of binding by the metallointercalator has been profitably exploited in characterizing how complexes bind DNA with specificity, as well as high affinity.

2.3.1. Recognition of 5′-Py–Pu-3′ Sites

One of the most extensively characterized and studied metal complexes that intercalates into DNA is $[Rh(phen)_2phi]^{3+}$.[53,55,56] In this mixed-ligand metallointercalator, the phenanthroline ligands provide structural form to the complex and the phi ligand serves to intercalate into the base stack of DNA by overlapping extensively with the π-stacked base pairs. In fact, it is the shape of this complex, with phenanthroline ligands that occlude part of the phi, that dominates its interactions with DNA.

We observed in early studies that $[Rh(phen)_2phi]^{3+}$ binds to DNA with moderate site selectivity, whereas little specificity was evident with a close analogue, $[Rh(phi)_2bpy]^{3+}$.[53] We proposed that the site selectivity of $[Rh(phen)_2phi]^{3+}$ was based upon shape selection. Because the steric bulk of the ancillary phenanthroline ligands blocks a portion of the phi aromatic surface, the complex could be considered to bind tightly only at sites which were more open in the major groove.[53,56] We also observed enantioselectivity favoring the Δ-isomer.[55] It was certainly interesting to observe even moderate site selectivity for this complex which lacked hydrogen bond donors or acceptors on the ancillary ligands.

Further study indicated that $[Rh(phen)_2phi]^{3+}$ showed a preference for sites with high propeller twisting toward the major groove.[55,57] The metal complex preferentially cleaves at 5′-YYR-3′ (where Y is pyrimidine and R is purine) sites, occasionally cleaves DNA at 5′-RYR-3′ sequences, but never cleaves at sequences of the form 5′-RRY-3′. Comparison of crystal structures of three B-form DNA oligonucleotides to the photocleavage patterns for $[Rh(phen)_2phi]^{3+}$ enabled the determination of the critical structural features for recognition.[57] Helical twist, rise, tilt, and roll, among other factors, were ruled out as important parameters. It was proposed that the propeller twisting allows the shape selection by opening up the B-form DNA purines in 5′-YYR-3′ dramatically, thus permitting facile intercalation of the phi ligand while simultaneously removing the counterpart pyrimidines from positions that would sterically clash with the phenanthroline rings of the metal complex (Figure 9). In contrast, a 5′-RRY-3′ site not only closes the major groove, but also places the pyrimidines in a highly unfavorable position with respect to the phenanthroline rings. $[Ir(phen)_2phi]^{3+}$ has been shown to have similar sequence specificity.[58]

As mentioned above, $[Rh(phi)_2bpy]^{3+}$ shows almost no sequence or structure selectivity.[56,59] Inspection of the geometry of this metal complex shows that the nonintercalating phi ligand is positioned away from possible steric clashes with the helix, as is the bpy ligand. Simple comparison of the shapes of these two metal complexes, therefore, highlights the idea that steric clashes, or their avoidance, can dominate site selectivity.

2.3.2. $[Rh(phen)_2phi]^{3+}$ as a Probe of RNA Structure

The observation that the site selectivity for $[Rh(phen)_2phi]^{3+}$ depends on somewhat open major grooves has been used most advantageously in probing RNA structures. We have seen repeatedly that our metallointercalators which targeted major groove sites bind poorly to double-stranded RNA.[60−62] We interpreted this observation based upon the fact that A-form RNA duplexes contain a very deep and narrow major groove, which would be largely inaccessible for stacking by the metal complex. Changes in tertiary structure of the RNA that serve to open the major groove are possible targets for the rhodium complex. This notion of shape-selective recognition by $[Rh(phen)_2phi]^{3+}$ led to the development of a novel probe for RNA tertiary structure. We examined first the interactions of the rhodium complex with an RNA

of well-characterized structure, tRNA, and thereafter applied our understanding of its recognition characteristics to probe other folded RNAs.

We found first that, with photoactivation, [Rh(phen)$_2$phi]$^{3+}$ promotes strand cleavage at sites of tertiary interaction in tRNA.[60,63] The rhodium complex yielded no cleavage in double-helical regions of the RNA nor in unstructured single-stranded regions. Instead, [Rh(phen)$_2$phi]$^{3+}$ appeared to target regions which are structured so that the major groove is open and accessible for stacking, as occurs where bases are triply bonded. Cleavage studies were conducted on two structurally characterized tRNAs, tRNA^{Phe} and tRNA^{Asp} from yeast, the unmodified yeast tRNA^{Phe} transcript, a chemically modified tRNA^{Phe}, as well as a series of tRNA^{Phe} mutants.[61] What we observed was that there was a striking similarity in cleavage on these tRNAs and the sites of cleavage marked regions of tertiary folding. Moreover, cleavage results on mutants indicated that it is the structure of the triply bonded array rather than the individual nucleotides that were being targeted.

We also carried out analogous experiments on tDNA^{Phe}, the DNA analogue of tRNA^{Phe}.[64] Although there were slight differences in photocleavage reactivity within the putatively tertiary regions, within the double-stranded regions of the stem regions of tDNA^{Phe} we observed strong photocleavage at 5′-YYR-3′ sites, as is expected for B-form DNA. Notably, these sites were not cleaved in the case of tRNA^{Phe}, consistent with the A-form nature of the tRNA stem. Perhaps most importantly, the similarity in pattern at sites of tertiary interaction in tRNA indicated that the tDNA adopted a similarly folded structure.

We next examined the three-dimensional folding of *Xenopus* oocyte 5S rRNA using [Rh(phen)$_2$phi]$^{3+}$ as a structural probe.[65] The sites targeted by the rhodium complex were mapped on the wild type *Xenopus* oocyte RNA, on a truncated RNA representing an arm of the molecule, as well as on several single-nucleotide mutants of the 5S rRNA. Given the similarity observed in cleavage between the full 5S RNA and the truncated fragment, our results did not support folding models which involved long-range tertiary interactions. Cleavage results with [Rh(phen)$_2$phi]$^{3+}$ did, however, indicate that the apposition of several noncanonical bases as well as stem-loop junctions and bulges could result in intimately stacked structures with opened major grooves. We suggested that these distinctive structures might also be utilized for specific recognition by proteins.

The strong interactions [Rh(phen)$_2$phi]$^{3+}$ showed with Hoogsteen-bonded triple-base sites prompted a systematic investigation of the recognition that this complex shows toward synthetic triple helices.[66] Consistent with the recognition seen on tRNA, we found that the metal complex interacts with triple helices in a structure-specific manner. Different cleavage patterns were seen with the Y·R−Y and R·R−Y motifs; cleavage was seen on both of the Watson−Crick strands of the former motif and primarily on the purine Watson−Crick strand of the latter motif with little cleavage on the Hoogsteen strand for either motif. Importantly, the metal complex showed no detectable cleavage on the A-form RNA duplex in the absence of the third Hoogsteen strand. Thus, the cleavage patterns were consistent with an intercalated model for the metal complex in the triple helix.

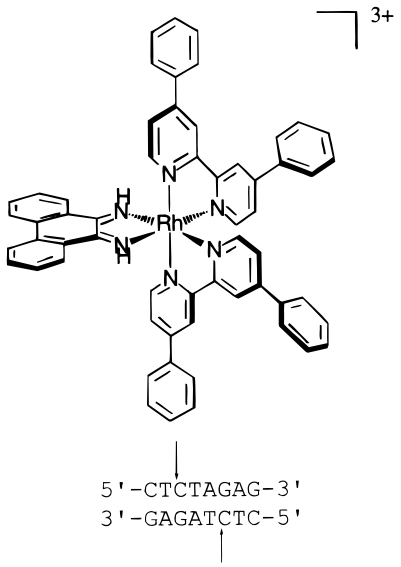

Figure 10. [Rh(DPB)$_2$phi]$^{3+}$ and the palindromic sequence recognized by cooperative binding of a noncovalent dimer. The arrows indicate the sites of photocleavage.

Last, we examined the Tat-binding site of the bovine immunodeficiency virus TAR RNA hairpin using [Rh(phen)$_2$phi]$^{3+}$ as a photochemical probe.[67] The primary site cleaved by the rhodium complex, upon photoactivation, was found to be U24, a base which participates in the novel base triple (with bases A13 and U10) characteristic of this folded RNA. In mutants where the RNA oligomer was unable to form the base triple, site-specific cleavage by the rhodium complex was abolished. Moreover, [Rh(phen)$_2$phi]$^{3+}$ was found to inhibit specific binding of BIV−Tat peptide to its target site. Thus, the rhodium complex, in matching its shape to the opened major groove of the properly folded RNA, could not only target a functionally important site on a folded RNA, but could compete for binding with a functionally important Tat peptide.

2.3.3. Site-Specific Recognition of a Palindromic Octamer by [Rh(DPB)$_2$phi]$^{3+}$

Perhaps the most striking example of site-specific recognition by shape selection with bulky ancillary ligands was found in the enantiospecific targeting of an eight-base pair site by Δ-[Rh(DPB)$_2$phi]$^{3+}$ (DPB = 4,4′-diphenylbpy).[59,68] In doing so, this metallointercalator was found to mimic different aspects of DNA-binding proteins (Figure 10). Specific photocleavage was induced by Δ-[Rh(DPB)$_2$phi]$^{3+}$ at the highlighted cytosine in the self-complementary sequence 5′-CT*C*TAGAG-3′; in contrast, Λ-[Rh(DPB)$_2$phi]$^{3+}$ yielded no detectable photocleavage, even at concentrations 1000-fold higher. Additionally, a distinct footprint was observed at the 5′-CTCTAGAG-3′ site for Δ-[Rh(DPB)$_2$phi]$^{3+}$ but not for Λ-[Rh(DPB)$_2$phi]$^{3+}$.

Significantly, as a monomer, the metal complex is geometrically capable of spanning only six base pairs. Thus, as with many DNA-binding proteins, specificity for the palindromic site appeared to depend on

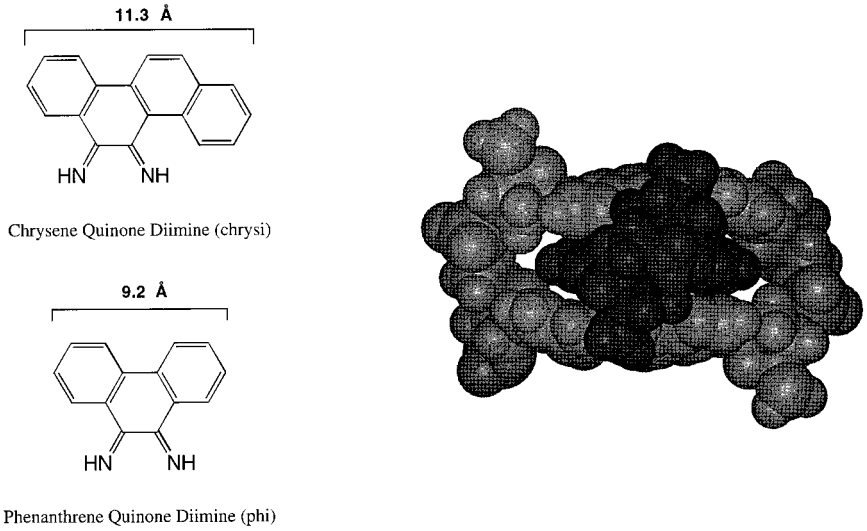

Figure 11. Comparison in size of chrysi and phi ligands (left), and illustration of a DNA binding site (right) containing Δ-α-[Rh[(R,R)Me_2trien]phi]$^{3+}$. The phi ligand fits snugly between the base pairs.

dimerization. The palindromic target site could be considered as two overlapping 5′-CTCTAG-3′ monomer sites on opposing strands; simultaneous intercalation into the central 5′-CT-3′ step of each monomer by Δ-[Rh(DPB)$_2$phi]$^{3+}$ would allow pendant phenyl groups from separate complexes to overlap over the central 5′-TA-3′ base step. Evidence for this cooperative mechanism was obtained by comparing the binding curves between an isolated monomer of 5′-CTCTAG-3′ with Δ-[Rh(DPB)$_2$phi]$^{3+}$ and the palindromic 5′-CTCTAGAG-3′. An enhancement of binding affinity for the palindromic site was observed, supporting a cooperative interaction of 2 kcal between metal complexes within the 8-mer site.

On the basis of these observations and the remarkable specificity observed, Δ-[Rh(DPB)$_2$phi]$^{3+}$ was then used to inhibit successfully XbaI restriction endonuclease activity at the palindromic site. No comparable inhibition was observed with a sequence-neutral DNA-binding metal complex nor with [Rh(DPB)$_2$phi]$^{3+}$ in competition with a restriction enzyme that binds an alternate site. Thus, a synthetic metallointercalator was found to bind to DNA with a level of specificity mimicking DNA-binding proteins and, in so doing, to inhibit site-specifically the reaction of a DNA binding protein.

2.3.4. [Rh(bpy)$_2$chrysi]$^{3+}$ Complexes and Mismatch Recognition

Among the most recent of the metallointercalators explored as probes of DNA structure is [Rh(bpy)$_2$chrysi]$^{3+}$ (chrysi = 5,6-chrysenequinone diimine).[69,70] This metal complex utilizes a somewhat different approach to DNA recognition. Here recognition is still based upon steric exclusion but now of the *intercalating* ligand. The strategy for shape-selective recognition of mismatched sites, irrespective of sequence, is based on the idea that expanding the size of the intercalating ligand by one aromatic ring might restrict access to normal B-DNA but retain access to destabilized mismatches; the size of the chrysi aromatic ring could make it too sterically bulky to insert into standard B-form DNA (Figure 11).

This strategy holds, to first order. Specific DNA cleavage by [Rh(bpy)$_2$chrysi]$^{3+}$ is observed at over 80% of mismatch sites in all possible single base pair sequence contexts around the mispaired bases. Significantly, a correlation exists between the stability of the mismatch and the ability of the metal complex to photocleave the mismatch site. Moreover, the affinity of the metal complex for a CA mismatch exceeds by almost 3 orders of magnitude that of the metal complex for nonspecific B-form DNA.

This extremely high selectivity of [Rh(bpy)$_2$chrysi]$^{3+}$ for base mismatches has been demonstrated also by targeting a single mismatch within a 2725 bp plasmid[70] (Figure 12). Following linearization of the two plasmids which differed in a sequence by only a single base, strands were mixed and reannealed in equimolar concentrations to form a 2.7 kilo-base pair DNA strand with a single mismatch at a known site. Low-resolution mapping of this construct after irradiation with the metal complex showed cleavage of the DNA into a 974 bp fragment and a 1751 bp fragment, the appropriate sizes for scission at the mismatch site. Higher resolution mapping confirmed that the metal complex was binding exclusively to the mismatch site. Sterically demanding intercalators such as [Rh(bpy)$_2$chrysi]$^{3+}$ may have application both in mutation detection systems and as mismatch-specific chemotherapeutic agents.

2.4. Direct Readout of DNA Functionality in the Major Groove

2.4.1. Rhodium Amine Complexes as Intercalators

The ability of an octahedral metallointercalator to contact functionalities within the major groove by direct hydrogen bonding and/or specific van der Waals contacts between the ancillary ligands and the DNA bases provides another strategy for site recognition. By designing metal complexes with functionality complementary to those of the base pairs arrayed three-dimensionally in the major groove, specificity can be achieved. Moreover, unlike shape selection, in targeting B-DNA sites, site-specific

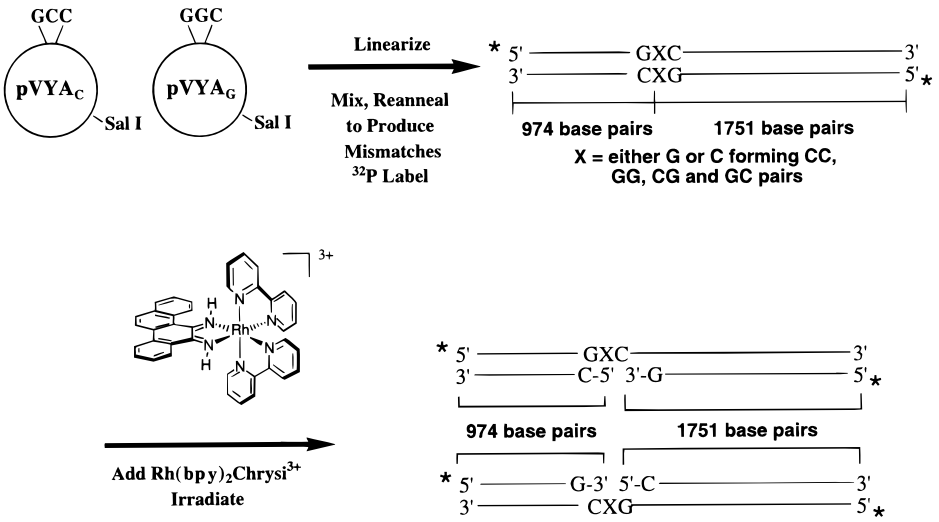

Figure 12. Experiment to test sensitivity of [Rh(bpy)$_2$chrysi]$^{3+}$ to detect a single mismatch in a 2.7 kbase pair DNA strand. Two plasmids with a single base difference were linearized by a restriction enzyme, mixed, and reannealed. The mixture of strands, including those which now contain a mismatch, was then irradiated with UV light in the presence of [Rh(bpy)$_2$chrysi]$^{3+}$ and examined by gel electrophoresis to test for site-specific cleavage.

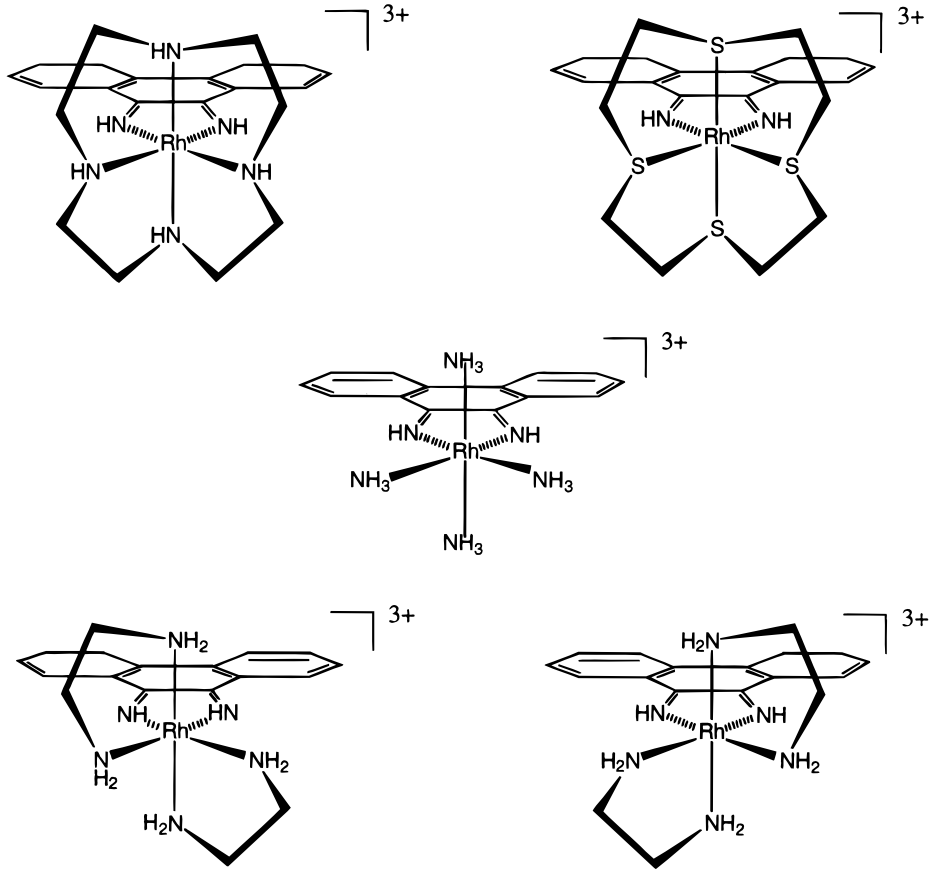

Figure 13. Phi complexes of Rh(III) with aliphatic ancillary ligands: (top left) [Rh[12]aneN$_4$phi]$^{3+}$; (top right) [Rh[12]-aneS$_4$phi]$^{3+}$; (center) [Rh(NH$_3$)$_4$phi]$^{3+}$; (bottom left) Λ-[Rh(en)$_2$phi]$^{3+}$; (bottom right) Δ-[Rh(en)$_2$phi]$^{3+}$.

metal complexes have the promise of being designed using this strategy with a level of predictability.

A family of rhodium amine complexes which contained the phi ligand was synthesized, and their selectivities for different sites were tested[71,72] (Figure 13). It was found that [Rh(NH$_3$)$_4$phi]$^{3+}$, [Rh(en)$_2$phi]$^{3+}$, and [Rh[12]aneN$_4$phi]$^{3+}$ cleave strongly at 5′-GC-3′ sites. Given the rigid structures of these complexes and the ability to orient the complexes on the DNA helix by intercalation, models were made which indicated the possibility of hydrogen bond formation between the axial amines of the metal complexes and the O6 of guanine: the C2 symmetry of the complexes would confer recognition of a 5′-GC-3′ base step. [Rh-[12]aneS$_4$phi]$^{3+}$, a control metal complex which lacks H-bond capability, was tested in parallel experiments and was seen to bind at alternate sites.

Additional experiments using these phi complexes of rhodium which contain axial amines probed hydrogen bonding to guanine through the introduction

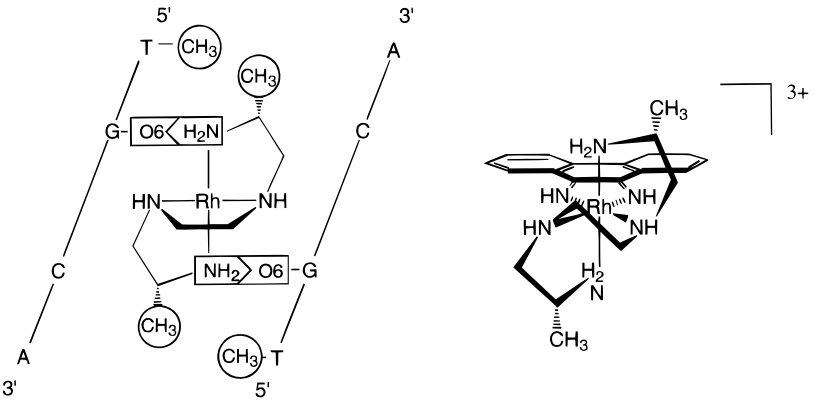

Figure 14. Schematic illustration of Δ-α-[Rh[(R,R)Me$_2$trien]phi]$^{3+}$ (right) and the proposed interactions with the 5′-TGCA-3′ intercalation site (left). The site-specific design was based upon potential van der Waals interactions between thymine methyl groups and pendant methyl groups on the complex backbone, as well as hydrogen bonding interactions between axial amines of complex and the O6 of guanine.

of O6-methyl guanine in place of guanine on the targeted oligonucleotide.[73,74] As expected, this modification disrupted binding to the site. In contrast, replacement of guanine with 7-deazaguanine did not disrupt recognition, suggesting that hydrogen bonding to the N7 of guanine is not an important factor in binding of these metal complexes. A related finding was that the Λ-[Rh(en)$_2$phi]$^{3+}$ enantiomer also bound to 5′-TX-3′ sites, especially 5′-TA-3′, due to a van der Waals contact between the methylene groups on the backbone of the complex and the thymine methyl; the Λ-isomer of the complex showed no such preference in binding. Mutation of the thymine to deoxyuracil, which lacks the methyl group, abrogated binding of Λ-[Rh(en)$_2$phi]$^{3+}$ to the 5′-TX-3′ sites.

2.4.2. Predictive Design and Direct Readout by Δ-α-[Rh[(R,R)-Me$_2$trien]phi]$^{3+}$

Using the basic characterization of potential noncovalent contacts between phi intercalators containing amine ligands, a new complex, Δ-α-[Rh[(R,R)-Me$_2$trien]phi]$^{3+}$, was designed specifically to bind to a 5′-TGCA-3′ site[75] (Figure 14). The targeting of this site was based upon predicted hydrogen bonding contacts between the axial amines and the O6 of guanine, as well as potential van der Waals contacts between the pendant methyl groups on the metal complex and the methyl groups on the flanking thymines.[71] Photocleavage data indicated that the complex binds to the target site with a binding constant of 9×10^7 M^{-1}.[76] A high-resolution NMR structure[41,76] and, recently, a crystal structure of the metal complex intercalated through the major groove[42] all confirm that this complex targets the sequence 5′-TGCA-3′ from the major groove and, remarkably, that each of the predicted contacts are present.

The crystal structure of the rhodium intercalator Δ-α-[Rh[(R,R)-Me$_2$trien]phi]$^{3+}$ bound specifically to the central 5′-TGCA-3′ site of an eight-base pair DNA oligonucleotide was solved at 2.0 Å resolution and represents the first crystallographically characterized high-resolution view of a metallointercalator bound to a DNA duplex[42] (Figure 15). Five intercalated DNA duplexes in the asymmetric unit provide crystallographically independent views of the detailed interactions between the intercalator and the major groove binding site. The structure shows that the base pairs are well stacked, the phi ligand is deeply intercalated, and the conformation of the deoxyribose sugars at the intercalation site is B-form. Indeed, metallointercalation here causes minimal structural perturbation to DNA. Essentially the intercalator resembles an inserted base pair. This structure provides a rational basis for expanding the current repertoire of sequence-specific intercalators and fundamental support for the strategy of utilizing octahedral metallointercalators in predictable site-specific design.

2.4.3. Rhodium Complex–Peptide Chimeras

An entirely different strategy toward designing DNA binding agents utilizes a metallointercalator to provide nonspecific affinity for DNA within a larger assembly of recognition elements. Proteins often use a significant percentage of their amino acids to provide a scaffold that has high nonspecific affinity for DNA and an appreciably smaller number of amino acids to contact the base pairs directly. In an effort to construct a complex with the nonspecific affinity of the metallointercalator and less steric bulk and complexity than the full DNA-binding protein, while trying to maintain the essential site recognition characteristics of the original peptide motif, a derivative of [Rh(phi)$_2$bpy]$^{3+}$ was coupled to a peptide whose sequence was derived from the contact region in a DNA binding protein.[77]

Another example of this strategy in which a high level of site specificity was obtained used the 13 amino acid DNA binding domain of phage P22 repressor coupled to [Rh(phi)$_2$bpy′]$^{3+}$ [78] (Figure 16). Systematic variations in this motif revealed that the recognition characteristics of this molecule were critically dependent on a single glutamate. In cases where the glutamate was present, even with variations within the surrounding sequence, the chimera specifically recognized 5′-CCA-3′. However, changes as conservative as replacing glutamate with the isostere glutamine or shortening the side-chain group by one methylene, replacing glutamate with aspartate, entirely destroyed the recognition characteristics of this metallointercalator. CD studies indicated that this glutamate was essential to maintain the

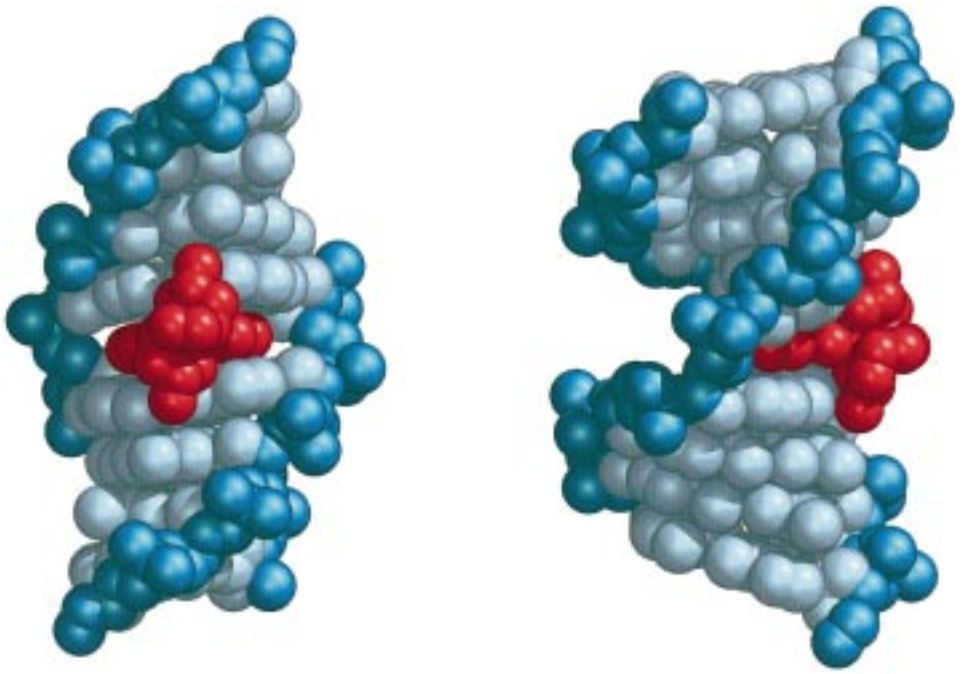

Figure 15. Two views (rotated by 90°) of the crystal structure of Δ-α-[Rh[(R,R)Me_2trien]phi]$^{3+}$ bound to 5′-GTTGCAAC-3′. The metal complex is depicted in red, and the DNA double helix is in blue.

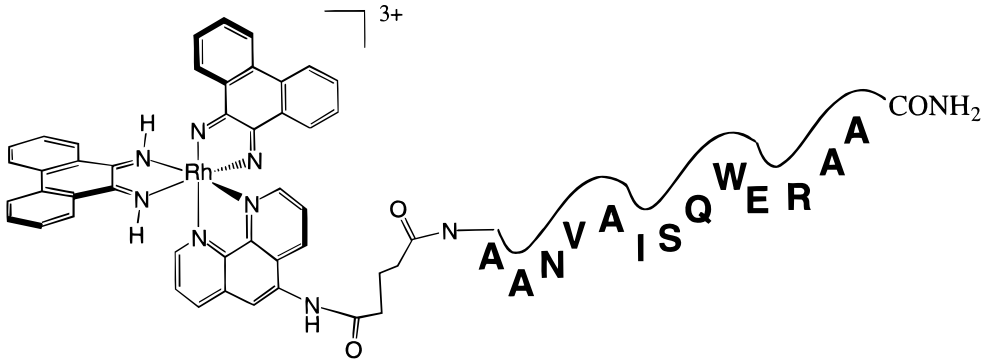

Figure 16. A [Rh(phi)$_2$phen′]$^{3+}$−peptide chimera.

α-helicity of the peptide; its removal disrupted the structure significantly. Hence, glutamate was proposed to act as a switch for recognition in this system and its absence destroyed both the secondary structure within the chimera peptide backbone and the DNA recognition of the ensemble.

Important issues still need to be established in effecting this design strategy. The metallopeptides lack rigidity and often predictability in their structure. Moreover, the relationship between the peptide conformation in the chimera versus that in the parent DNA-binding protein is also not necessarily strong. As such, while the construction of metallointercalating-peptide chimeras offers a whole new array of molecules to explore for site-specific recognition, challenges remain in achieving predicable site-specificity with these complexes.

2.5. Combining Direct Readout and Shape Selection

2.5.1. Site-Specific Recognition by Λ-1-[Rh(MGP)$_2$phi]$^{5+}$

[Rh(MGP)$_2$phi]$^{5+}$, a derivative of [Rh(phen)$_2$phi]$^{3+}$ containing pendant guanidinium groups on the phenanthroline ligand, was designed to target a subset of sites recognized by [Rh(phen)$_2$phi]$^{3+}$.[79,80] Because MGP (MGP = 4-(guanidylmethyl)-1,10-phenanthroline) is an asymmetric ligand, condensation of the ligand into two positions of an octahedral metallointercalator affords three possible positional isomers, each of which has two enantiomers (Figure 17). On the basis of modeling, it was predicted that 1-[Rh(MGP)$_2$phi]$^{5+}$ would target the subset of [Rh(phen)$_2$phi]$^{3+}$ sites that were flanked by G·C base pairs due to the potential hydrogen bonding to guanine sites that the MGP ligand afforded when this isomer was oriented along the major groove of DNA.

Δ-1-[Rh(MGP)$_2$phi]$^{5+}$ was indeed found to target 5′-CATCTG-3′ specifically, and NMR experiments showed that it binds to the target site in two modes canted from each other in the central base step.[81] Remarkably, however, the Λ-isomer also showed site specificity. Λ-1-[Rh(MGP)$_2$phi]$^{5+}$ recognized the sequence 5′-CATATG-3′ with high site selectivity and affinity; systematic replacement of the bases in this consensus sequence showed that variation within this binding site caused a dramatic reduction in binding.[79] Since initial modeling studies had shown no possible

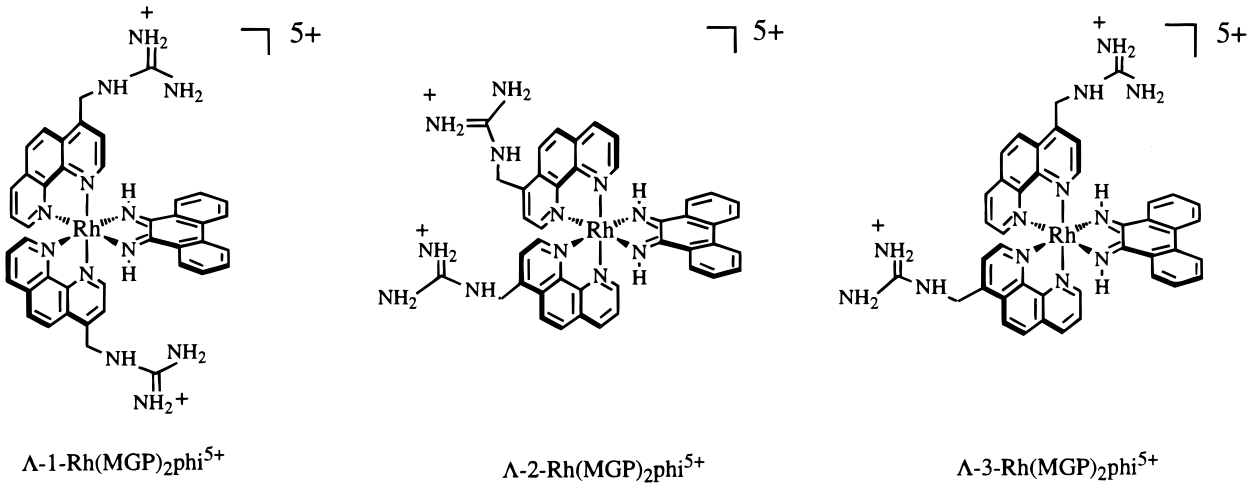

Figure 17. Three configurational isomers of $[Rh(MGP)_2phi]^{5+}$.

specific interactions within a normal B-form site due to the left-handed symmetry of this metal complex, it was difficult to understand how this complex could bind B-DNA at all.

Additional modeling showed that specific binding to a six-base pair sequence by Λ-1-$[Rh(MGP)_2phi]^{5+}$ was possible only if the complex bound to a significantly unwound DNA site, essentially flattening the helix into a ladder at the binding site.[79] Plasmid unwinding assays were devised to test for this site-specific unwinding and indeed established that the complex bound to a DNA site marked by 70° unwinding. NMR studies provided additional support for this binding model.[81] It is in this conformation that the complex can span the entire six-base pair binding site and contact the N7 position of the flanking guanines with the pendant guanidinium groups. Importantly, experiments that replaced these flanking guanines with deazaguanine showed that the absence of the N7 nitrogen removed selectivity for the site, as seen by both NMR studies and photocleavage.[81]

We proposed then that the complex targeted its site by a combination of direct readout and shape selection. While hydrogen bonding to guanine positions was critical, also important was the propensity of the 5′-ATAT-3′ site for flexibility or "twistability". This explains the complete loss of recognition for the less flexible sequence 5′-CACGTG-3′. NMR studies additionally supported the trapping of the target site by the complex in an unwound conformation. It is notable that this complex, in contrast to most other complexes described here, showed a higher binding affinity by the Λ-isomer for its target site ($\sim 10^{-8}$ M^{-1}) than did the Δ-isomer for its site ($\sim 10^{-7}$ M^{-1}). This combination of shape-selection and direct readout can be powerful and highly specific.

2.5.2. Λ-1-[Rh(MGP)$_2$phi]$^{5+}$ as an Inhibitor of Transcription Factor Binding

Given its high affinity and specificity, Λ-1-$[Rh(MGP)_2phi]^{5+}$ has additionally been used to inhibit site specifically a transcription factor from binding to a modified activator recognition region[82] (Figure 18). In competition experiments with yeast Activator Protein 1 (yAP-1), the metal complex was able to compete with the protein for a binding domain that

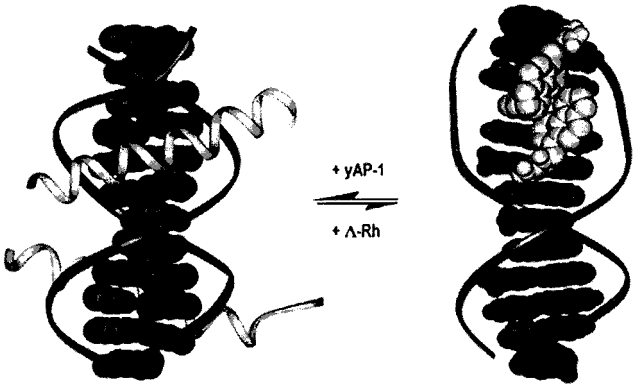

Figure 18. Illustration of the inhibition of transcription factor yAP-1 by Λ-1-$[Rh(MGP)_2phi]^{5+}$.

included both a yAP-1 binding region and a Λ-1-$[Rh(MGP)_2phi]^{5+}$ binding site. The concentration of metal complex required for this site-specific inhibition was 120 nM. The use of the parent complex, $[Rh(phen)_2phi]^{3+}$, in identical competition experiments required over 3 orders of magnitude more metal complex to afford the same competitive disruption of protein gel shift. This reaction was additionally seen to be isomer specific, as the symmetric isomer 3-$[Rh(MGP)_2phi]^{5+}$, in which the guanidinium groups are projected away from the phi ligand, showed no competitive binding with the protein. These results demonstrated the utility of metallointercalators not only as biochemical probes of nucleic acid structures but also, potentially, as therapeutic agents in gene regulation.

3. Reactions of DNA by Metallointercalators

Since metal complexes lend themselves to many spectroscopic techniques, their utility as spectroscopic probes in biological systems has been the subject of an increasing amount of study. However, transition-metal complexes offer also a rich reactivity, particularly in the context of redox chemistry, and this chemistry can be harnessed with metallointercalators to yield a treasure trove of reactions with DNA. It is, in fact, this reactivity that helped in establishing the site specificity of many of the metallointercalators, as already described. Indeed, the redox reactiv-

ity of even nonspecifically bound metallointercalators can be used in footprinting assays to determine the sequence preference of other DNA-binding molecules. The first such footprinting agent was MPE−Fe(II), a complex constructed by bringing together an organic intercalator, ethidium, and a redox-active metal complex, FeEDTA.[83]

Here we highlight some of the different reactions of coordinatively saturated metallointercalators with DNA. As reactive species, noncovalently bound metallointercalators can be used advantageously in probing DNA. Significantly, intercalation itself can provide a path to reactivity not available to complexes that are not well stacked in DNA.

3.1. Direct Oxidative Strand Cleavage: Reactions with the Sugar

Many DNA binding agents degrade DNA in a mechanism involving abstraction of a hydrogen atom from a sugar adjacent to the binding site. Minor groove binding molecules such as bis(1,10-phenanthroline)copper(I), Fe(II)·bleomycin, and metal-centered porphyrins all display direct DNA strand scission consistent with hydrogen abstraction from the C1′, C4′, and C5′ of the deoxyribose ring, and studies of the reactivity by these molecules have been the subject of a recent review.[84] C3′ and C2′ hydrogen atoms are instead accessible for attack by complexes that bind in the major groove, but because there are very few oxidative cleaving agents which bind to DNA via the major groove, there has been little opportunity to study this reaction. Phi complexes of Rh(III), as major groove intercalators, fit this binding requirement, and their photoinduced strand-cleaving reactivity has thus been the subject of some study. This reactivity is seen to be quite distinctive from that of alternate DNA-damaging agents.

It was first proposed that ultraviolet irradiation of an intercalated phi complex of Rh(III) leads to the generation of a radical on the phi ligand via ligand-to-metal charge transfer.[56] We proposed that the ligand radical then can abstract a C3′ hydrogen from the adjacent deoxyribose; as a result, the sugar radical would degrade, leading to DNA strand cleavage. Photolysis of $[Rh(phen)_2phi]^{3+}$ or $[Rh(phi)_2bpy]^{3+}$ bound to DNA does, in fact, yield DNA strand cleavage and, in the absence of O_2, results in the formation of 3′ phosphate and 5′ phosphate termini, as well as free bases. In the presence of oxygen, different products result; direct strand cleavage is observed, but products include, instead, the 5′ phosphate terminus, base propenoic acid, and a 3′ phosphoglycaldehyde end. By analogy with reactions of bleomycin at the C4′ position, these products of DNA degradation by phi complexes of Rh(III) are consistent with radical chemistry at the C3′ position. Recent NMR and crystallographic studies have indicated a close association between the phi ligand and the C2′, rather than the C3′, position, however.[41,42,76] Perhaps, then, the initial reaction of the photoexcited intercalator occurs with the C2′−H followed by H-migration to form the C3′ radical with subsequent degradation. More detailed analysis will be required to establish this mechanism precisely. Certainly it is the orientation of the metallointercalator within its major groove site that determines this chemistry. Intimate contact with DNA is required, and no diffusible radical species is involved in the DNA strand cleavage.

It should be noted here that much of what we know about how phi complexes of rhodium(III) recognize specific sites was derived first from DNA photocleavage experiments. Confirmation of recognition and greater structural definition would emerge later from NMR studies. Thus, despite the very low quantum yields for photocleavage by these complexes, the fact that reactivity was localized, not involving a diffusible species, and essentially independent of sequence (a characteristic of reactions on the deoxyribose ring) led to a valuable nucleic acid probe. In a straightforward fashion, this reactivity has been used generally to mark the sites of binding by rhodium intercalators.

3.2. Hydrolytic Strand Cleavage

The search for complexes that mimic DNA restriction enzymes by binding selectively to specific DNA sites and cleaving by hydrolysis of the phosphate has been the subject of a recent review.[85] Here, too, in the design of artificial nucleases, metallointercalators have been employed, in particular, a metallointercalator−peptide chimera. In our laboratory, an assembly containing a peptide tethered covalently to the $[Rh(phi)_2bpy]^{3+}$ was constructed to explore hydrolytic DNA cleavage.[86] In this strategy, once the metal complex was bound to DNA by intercalation of the phi ligand, the peptide was proposed to be delivered to the backbone of DNA for reaction rather than recognition and, furthermore, for a hydrolytic reaction on DNA rather than redox chemistry (Figure 19). The 16-residue peptide chain was designed de novo, based upon studies of the active sites of several metallic hydrolases. In this design the peptide has a propensity to adopt an α-helical conformation with two histidines on one face to coordinate a Zn^{2+}. It was hoped that delivery of the Zn^{2+} to the phosphodiester would yield hydrolytic reactivity on the sugar−phosphate backbone. Cleavage products of the complex were analyzed by gel electrophoresis, where control sequencing lanes were run alongside product lanes. Band migration of the cleavage products showed that the cleaved DNA termini contained hydroxyl ends, rather than phosphates. Moreover, the presence of only 3′ hydroxyl termini, rather than a mixture of terminal products, indicated that the peptide cleaves stereospecifically; this stereospecificity might be a result of the complex's major groove binding orientation.

In fact, the reactivity of this metallointercalator−peptide chimera represented a first step in the development of a true synthetic nuclease. While sequence specificity was not achieved by this assembly, the possibility remains that similar short peptides that are tethered to more specific intercalators can serve as synthetic, sequence-specific restriction enzymes.

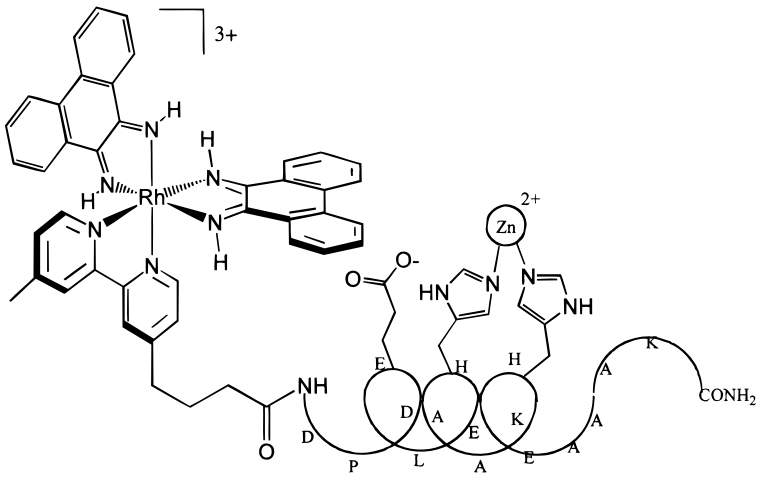

Figure 19. Schematic depiction of a metallointercalator−peptide chimera with coordinated Zn^{2+}. This complex has been shown to cleave DNA hydrolytically.[79]

3.3. Oxidative Reactions with the DNA Bases

Oxidative damage to DNA bases generally occurs at guanine, which has the lowest oxidation potential of all the DNA bases. Damage to this base does not cause direct strand scission, however, so reactions must be post-treated with piperidine or aniline in order to analyze the reactivity of the oxidants. The oxidative damage to DNA can occur by one of four mechanistic pathways: (i) by direct electron transfer from the guanine to a bound metal complex (we have already seen examples of such direct electron transfer in spectroscopic studies with potent photooxidants such as TAP and HAT complexes of ruthenium(II));[21] (ii) by oxo transfer (such reactions have been used in assays of base accessibility with intercalators well-stacked in the helix); (iii) as a result of reaction with singlet oxygen, which is formed upon sensitization of a DNA-bound metallointercalator (exploitation of damage by this pathway has been a basis for photochemotherapeutic strategies);[87] and (iv) over a long range via DNA-mediated electron transfer.[88]

3.3.1. Base Damage by Oxo Transfer

Many examples of DNA cleaving using Mn porphyrin activated with persulfate or other oxygen donors have been documented, and these yield oxidative damage both to the sugars and DNA bases.[89,90] Whether it is an intercalated metalloporphyrin that is reactive in these cases is not likely, however, since it is an axially bound oxo that is delivered to the DNA sugar or base.

Direct oxidation of DNA bases has also been accomplished by activation of Ru(II) complexes such as $[Ru(bpy)_3]^{2+}$ and *trans*-$[Ru(O_2)(4\text{-OMe-Py})_4]^{+}$ electrochemically.[91,92] Reactivity can be enhanced by coordinating an intercalating ligand, as with $[Ru(tpy)(dppz)O]^{2+}$,[93] but here too reaction is likely not from the intercalatively bound mode. Oxidative reaction is evident preferentially at guanines. This chemistry has been exploited as a probe of DNA and RNA hybridization.[92]

3.3.2. Guanine Oxidation by Singlet Oxygen

Singlet oxygen is well documented as a source of oxidative damage to DNA bases.[94] There are several examples of DNA-binding metal complexes that can generate singlet oxygen species via a triplet energy transfer from the excited state of a metal complex to $^3O_2$. Such reactions with DNA involving porphyrins, Ru(II) complexes of HAT, TAP, and bpz, and vanadium(V) complexes, are discussed in a recent review.[95]

We originally exploited the high efficiency of singlet oxygen sensitization by $[Ru(bpy)_3]^{2+}$ derivatives in probing A-form nucleic acids.[62,96] In these cases, while the metal complexes were not bound by intercalation, the $^1O_2$ generated locally by the surface-bound metal complex could be used to probe the location of the bound metal. Because the reactivity of singlet oxygen is so much higher with G as compared with T, A, and C and because $^1O_2$ can diffuse along the helix, the reaction is not a favored one in marking binding sites of metal complexes on DNA. Nonetheless, in the absence of alternative methods, such sensitization can be necessary. For ruthenium complexes, such reactions have been important to explore binding locations on the helix. Ruthenium(II) dppz complexes, for example, with shorter excited-state lifetimes than $[Ru(bpy)_3]^{2+}$ when bound to DNA, are only moderate sensitizers of $^1O_2$.[31] However, this reaction has proven to be critical in marking sites of intercalation of tethered dppz complexes along DNA oligonucleotides.[97]

3.3.3. Guanine Oxidation by Long-Range Electron Transfer

DNA-mediated electron transfer has been a much debated topic of research.[88] Of particular interest to this review is the exquisite sensitivity of DNA-mediated electron-transfer reactions to stacking. Hence, metallointercalators which are able to oxidize DNA bases are able to do so from a distance.

Oxidative damage to DNA by one-electron transfer occurs at G's, in particular at the 5′-G's of 5′-GG-3′ doublets. Calculations have shown that generally these guanines have a particularly low oxidation

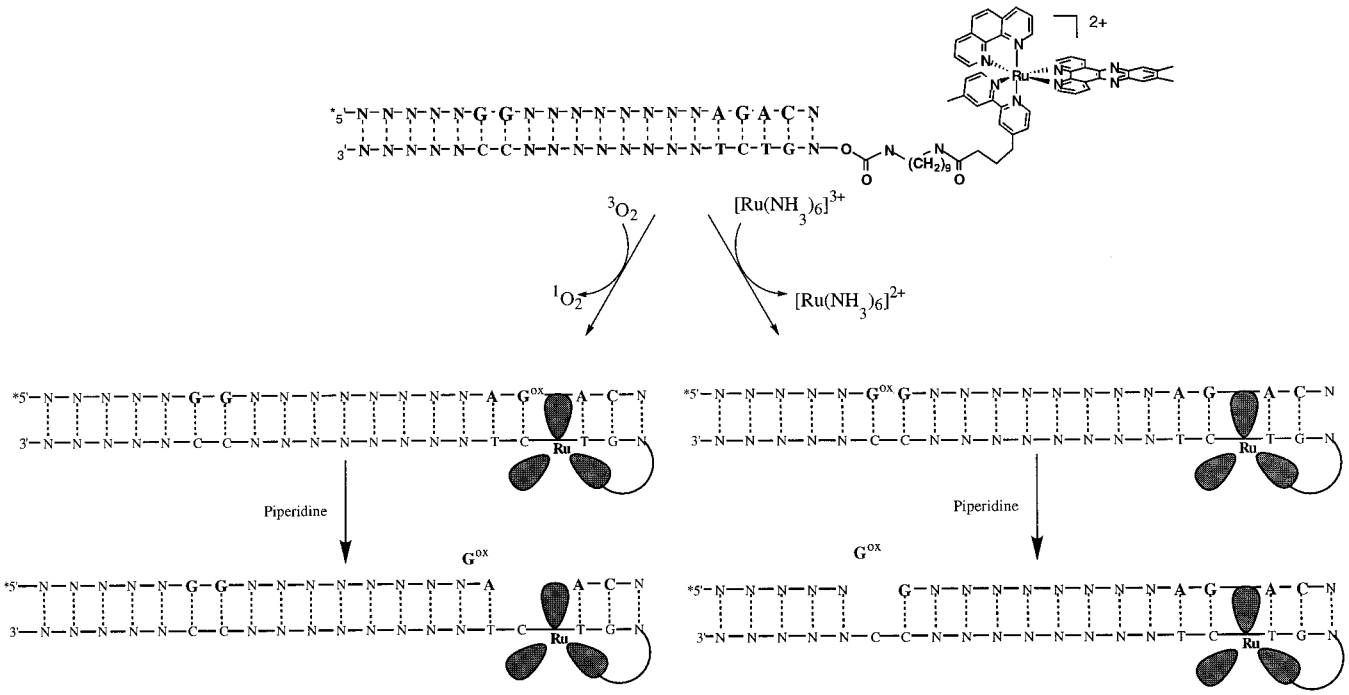

Figure 20. Singlet oxygen-dependent (left) and quencher-dependent (right) pathways to guanine oxidation by a covalently tethered $[Ru(phen)(dmb')(Me_2dppz)]^{2+}$ complex (top).[89]

potential.[98,99] Following one-electron oxidation, the guanine radical can react both with O_2 and H_2O to form a series of irreversible products, and some of these oxidation products can be revealed in biochemical experiments as strand cleavage events upon treatment with piperidine.[100] Interestingly, the piperidine-sensitive reaction of a range of species at the 5′-G of 5′-GG-3′ sites has come to be regarded as a signature for electron transfer to DNA.

Figure 20 illustrates two oxidative reactions of a Ru(II) intercalator tethered to DNA.[97] As mentioned above, photoexcited ruthenium(II) complexes can sensitize the formation of $^1O_2$, which can then react preferentially at nearby guanine residues, causing damage which marks the site of the binding. However, the photoexcited Ru(II) can also be quenched by electron transfer to a surface-bound quencher such as $[Ru(NH_3)_6]^{2+}$ or methyl viologen. Once quenched, the Ru(III) intercalator, generated in situ, becomes a potent ground-state oxidant. Ru(III) intercalators generated through this flash−quench technique can then be employed to damage DNA from a distance, by electron transfer, yielding reaction at the 5′-G of 5′-GG-3′ sites. This flash−quench methodology has also been exploited using noncovalently bound $[Ru(phen)_2dppz]^{2+}$ and poly-d(GC) to spectroscopically characterize the guanine radical formed in the DNA duplex.[101]

Damage to DNA sites from a distance was first demonstrated in assemblies containing a tethered phi complex of rhodium(III) as the photooxidant, which was spatially separated from the site of oxidation.[102] It had earlier been seen that low-energy photolysis of the complex produced a potent photooxidant (∼2 eV).[103] $[Rh(phi)_2bpy']^{3+}$ was covalently tethered to a 15-base pair strand of DNA and annealed to a complement which contained two 5′-GG-3′ sites, one 17 Å and one 34 Å from the intercalation site of the metal complex, well out of reach for direct electron transfer (Figure 21). The Rh−DNA assembly was first irradiated at 313 nm to induce direct strand cleavage, marking the site of rhodium intercalation near the tethered end. Rh−DNA samples were then irradiated at 365 nm, treated with hot piperidine, and examined by gel electrophoresis. Quantitation of the gel bands after photooxidation revealed that both the proximal and distal 5′-GG-3′ doublets were equally damaged, and controls showed that the reaction was intraduplex. Hence, this experiment established oxidative damage to DNA from a distance via long-range electron transfer. Preferential oxidation was seen with the Δ-diastereomer, consistent with the sensitivity of the reaction to the deep intercalation of the oxidant. Subsequent studies also showed the sensitivity of the reaction to the intervening base pair stack; assemblies containing bulges inserted in the DNA between the proximal and distal 5′-GG-3′ doublets showed a diminution in oxidation at the distal site.[104] Indeed, long-range oxidation was also shown to be modulated by proteins that bind DNA and perturb stacking at an intervening site.[105] In recent studies, damage has been reported at sites that are up to 200 Å away from the site of intercalation of the metal oxidant.[106]

3.3.4. Oxidative Repair of Thymine Dimers

The oxidative chemistry of rhodium intercalators has also been used to repair thymine dimers in DNA.[107,108] Here, too, the potency of the complex as a photooxidant was harnessed. The thymine dimer is the most common photochemical lesion in DNA, and it arises as a result of the 2 + 2 cycloaddition reaction between neighboring thymines on the same DNA strand upon photolysis with ultraviolet light. In bacterial cells, thymine dimers are repaired reductively by the enzyme photolyase, but model stud-

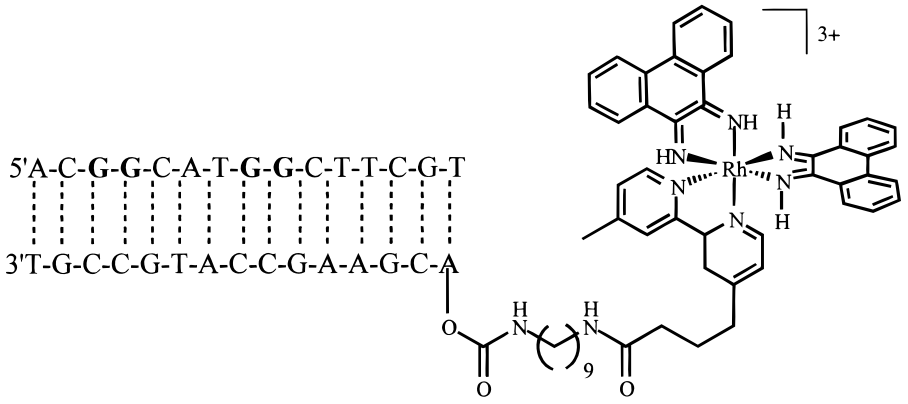

Figure 21. $[Rh(phi)_2bpy']^{3+}$ covalently tethered to a 15-mer with proximal (17 Å) and distal (34 Å) 5′-GG-3′ sites. 5′-G's were oxidized as a result of excitation of the intercalated complex (primarily between the 5′-TC-3′) followed by long-range electron transfer through the DNA base pair stack.

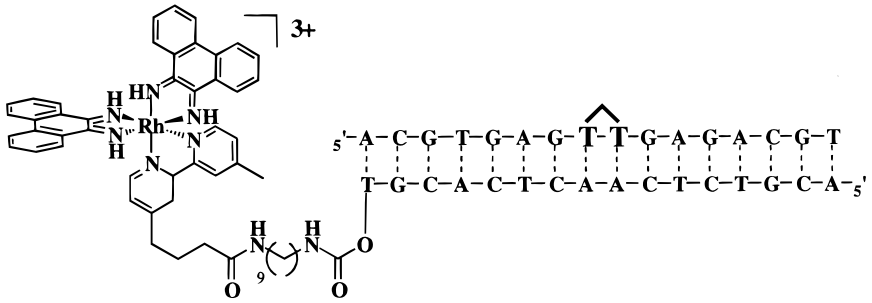

Figure 22. $[Rh(phi)_2bpy']^{3+}$ covalently tethered to a 16-mer oligonucleotide containing a thymine dimer lesion.

ies had shown that thymine dimers might also be repaired oxidatively.

DNA duplexes were synthesized containing a site-specifically incorporated thymine dimer and then photolyzed with visible light in the presence of noncovalently bound $[Rh(phi)_2bpy']^{3+}$.[107] High temperature HPLC showed the quantitative repair of the DNA promoted by the metal complex without any damage to the complementary strand. Moreover, only catalytic amounts of $[Rh(phi)_2bpy']^{3+}$ per DNA duplex were required, consistent with the oxidative repair mechanism. Indeed, quantitative repair could be seen with micromolar concentrations of $[Rh(phi)_2bpy']^{3+}$ and exposure of samples simply to sunlight.

The repair of thymine dimers in DNA by photolysis of the metallointercalators was next demonstrated at a distance with 16−19-base strands of DNA that contained a single TT sequence with no adjacent pyrimidines. These strands were irradiated with ultraviolet light to induce the thymine dimer lesion, and the damaged strand was then annealed to a complementary strand which contained a covalently tethered $[Rh(phi)_2bpy']^{3+}$ complex with an intercalation site 19−26 Å from the damage site (Figure 22). The damaged Rh−DNA assembly was then irradiated with light at 400 nm, and as $[Rh(phi)_2bpy']^{3+}$ oxidized the thymine dimer, the conversion from damaged to repaired DNA was monitored by HPLC. The repair efficiency of $[Rh(phi)_2bpy']^{3+}$ was about equal whether the complex was to the 5′ or to the 3′ side of the lesion. Several different lengths of DNA were used, and interestingly, the repair efficiency increased from 67% to 100% as the distance increased from 19 to 26 Å; perhaps this reflected the increased stability associated with stacking of the longer DNA duplexes. Another experiment introduced kinks into the DNA helix via extra, unpaired bases in order to determine if the disruption of the DNA π stack would affect the repair of the thymine dimer, which it did, reducing the repair efficiency by half. Here, too, then long-range electron transfer requires a well-stacked assembly.

4. Summary and Implications for the Future

Here we have seen many examples of reactions and site recognition by metallointercalators. Synthetic metallointercalators have been prepared with a diversity of functions, from luminescent probes for DNA, to structural probes of RNA, or photochemical reagents for thymine dimer repair. Complexes have been designed which target a diversity of sites on double-helical DNA, as well, whether through shape selection, direct read-out, or a combination. Indeed, even mismatches in DNA can now be targeted by metallointercalator recognition with high specificity. The utility of such metallointercalators as probes and diagnostic agents is evident.

However, much work needs to be done to develop the therapeutic potential of these complexes. Metallointercalators rank among the few synthetic complexes which target the DNA major groove with specificity, and indeed, we have already observed that such site-specific targeting can lead to the selective inhibition of DNA-binding proteins. But can such complexes traffic into a cell to inhibit transcription in vivo? Can such strategies for recognition be improved upon and generalized? Can we also apply DNA electron-transfer chemistry to probe and elucidate damage and repair of DNA within the cell?

Surely we have learned a great deal since our earliest studies of the chiral discrimination in binding octahedral complexes to DNA. We continue to be reminded much about the rich chemistry to be exploited with metallointercalators. They provide versatile shapes, a diversity of functionality, varied photophysical properties, and redox reactivity. The recognition and reactions of metallointercalators certainly promise to offer new tools to exploit as well as new challenges as we apply these probes to target nucleic acids within the cell.

5. Acknowledgments

We are grateful to the NIH (GM33309) for their financial support. We also thank our many co-workers and collaborators, as cited, as well as the many researchers from other laboratories who helped elucidate the chemistry of metallointercalators.

6. References

(1) Lerman, L. S. *J. Mol. Biol.* **1961**, *3*, 18.
(2) Jennette, K. W.; Lippard, S. J.; Vassiliades, G. A.; Bauer, W. R. *Proc. Natl. Acad. Sci. U.S.A.* **1974**, *71*, 3839.
(3) Barton, J. K.; Dannenberg, J. J.; Raphael, A. L. *J. Am. Chem. Soc.* **1982**, *104*, 4967.
(4) Barton, J. K.; Danishefsky, A. T.; Goldberg, J. M. *J. Am. Chem. Soc.* **1984**, *106*, 2172.
(5) Kumar, C. V.; Barton, J. K.; Turro, N. J. *J. Am. Chem. Soc.* **1985**, *107*, 5518.
(6) Barton, J. K.; Goldberg, J. M.; Kumar, C. V.; Turro, N. J. *J. Am. Chem. Soc.* **1986**, *108*, 2081.
(7) Barton, J. K.; Raphael, A. L. *Proc. Natl. Acad. Sci. U.S.A.* **1985**, *82*, 6460.
(8) Rehmann, J. P.; Barton, J. K. *Biochemistry* **1990**, *29*, 1701.
(9) Rehmann, J. P.; Barton, J. K. *Biochemistry* **1990**, *29*, 1710.
(10) Barton, J. K. *Science* **1986**, *233*, 727.
(11) Yamagishi, A. *J. Chem. Soc., Chem. Commun.* **1983**, 572.
(12) Satyanarayana, S.; Dabrowiak, J. C.; Chaires, J. B. *Biochemistry* **1992**, *31*, 9319.
(13) Satyanarayana, S.; Dabrowiak, J. C.; Chaires, J. B. *Biochemistry* **1993**, *32*, 2573.
(14) Eriksson, M.; Leijon, M.; Hiort, C.; Norden, B.; Graslund, A. *Biochemistry* **1994**, *33*, 5031.
(15) Pyle A. M.; Barton, J. K. In *Progress in Inorganic Chemistry: Bioinorganic Chemistry*; Lippard, S. J., Ed.; John Wiley & Sons: New York, 1990; Vol. 38, pp 413−475.
(16) Johann, T. W.; Barton, J. K. *Philos. Trans. R. Soc. (London)* **1996**, *354*, 299.
(17) Chow, C. S.; Barton, J. K. *Methods Enzymol.* **1992**, *212*, 219.
(18) Murphy, C. J.; Barton, J. K. *Methods Enzymol.* **1993**, *226*, 576.
(19) Holmlin, R. E.; Stemp, E. D. A.; Barton, J. K. *Inorg. Chem.* **1998**, *37*, 29.
(20) Friedman, A. E.; Chambron, J.-C.; Sauvage, J.-P.; Turro, N. J.; Barton, J. K. *J. Am. Chem. Soc.* **1990**, *112*, 4960.
(21) Moucheron, C.; Kirschdemesmaeker, A.; Kelly, J. M. *J. Photochem. Photobiol. B* **1997**, *40*, 91.
(22) Carlson, D. L.; Huchital, D. H.; Mantilla, E. J.; Sheardy, R. D.; Murphy, W. R. *J. Am. Chem. Soc.* **1993**, *115*, 6424.
(23) Turro, C.; Bossmann, S. H.; Jenkins, Y.; Barton, J. K.; Turro, N. J. *J. Am. Chem. Soc.* **1995**, *117*, 9026.
(24) Olson, E. J. C.; Hu, D.; Hormann, A.; Jonkman, A. M.; Arkin, M. R.; Stemp, E. D. A.; Barton, J. K.; Barbara, P. F. *J. Am. Chem. Soc.* **1997**, *119*, 9, 11458.
(25) Moucheron, C.; Kirsch-De MesMaeker, A.; Choua, S. *Inorg. Chem.* **1997**, *36*, 584.
(26) Jacquet, L.; Kirsch-De MesMaeker, A *J. Chem. Soc., Faraday Trans.* **1992**, *88*, 2471.
(27) Arkin, M. R.; Stemp, E. D. A.; Holmlin, R. E.; Barton, J. K.; Hormann, A. E.; Olson, E. J. C.; Barbara, P. F. *Science* **1996**, *273*, 475.
(28) Tysoe, S. A.; Morgan, R. J.; Baker, D.; Strekas, T. C. *J. Phys. Chem.* **1993**, *97*, 1707.
(29) Hartshorn, R. M.; Barton, J. K. *J. Am. Chem. Soc.* **1992**, *114*, 5919.
(30) Holmlin, R. E.; Barton, J. K. *Inorg. Chem.* **1995**, *34*, 7.
(31) Holmlin, R. E.; Yao, J. A.; Barton, J. K. *Inorg. Chem.* **1999**, *38*, 174.
(32) Arounaguiri, S.; Maiya, B. G. *Inorg. Chem.* **1996**, *35*, 4267.
(33) Stoeffler, H. D.; Thornton, N. B.; Temkin, S. L.; Schanze, K. S. *J. Am. Chem. Soc.* **1995**, *117*, 7119.
(34) Yam, V. W.-W.; Lo, K. K.-W.; Cheung, K.-K.; Kong, R. Y.-C. *J. Chem. Soc., Dalton Trans.* **1997**, *3*, 2067.
(35) Jenkins, Y.; Friedman, A. E.; Turro, N. J.; Barton, J. K. *Biochemistry* **1992**, *31*, 10809.
(36) Tuite, E.; Lincoln, P.; Norden, B. *J. Am. Chem. Soc.* **1997**, *119*, 239.
(37) Hiort, C.; Lincoln, P.; Norden, B. *J. Am. Chem. Soc.* **1993**, *115*, 3448.
(38) Lincoln, P.; Broo, A.; Norden, B. *J. Am. Chem. Soc.* **1996**, *118*, 2644.
(39) Haq, I.; Lincoln, P.; Suh, D. C., Norden, B., Chowdhry, B. Z.; Chaires, J. B. *J. Am. Chem. Soc.* **1995**, *117*, 4788.
(40) Dupureur, C. M.; Barton, J. K. *J. Am. Chem. Soc.* **1994**, *116*, 10286.
(41) Hudson, B. P.; Barton, J. K. *J. Am. Chem. Soc.* **1998**, *120*, 6877.
(42) Keilkopf, C. L.; Erkkila, K. E.; Hudson, B. P.; Barton, J. K.; Rees, D. C. 1999. Submitted for publication.
(43) Dupureur, C. M.; Barton, J. K. *Inorg. Chem.* **1997**, *36*, 33.
(44) Greguric, I.; Aldrichwright, J. R.; Collins, J. G. *J. Am. Chem. Soc.* **1997**, *119*, 3621.
(45) Fry, J. V.; Collins, J. G *Inorg. Chem.* **1997,** *36*, 2919.
(46) Collins, J. G.; Sleeman, A. D.; Aldrich-Wright, J. R.; Greguric, I.; Hambley, T. W. *Inorg. Chem.* **1998**, *37*, 3133.
(47) Wang, A. H. J.; Nathans, J.; van der Marel, G.; van Boom, J. H.; Rich, A. *Nature* **1978**, *276*, 471.
(48) Fiel, R. J.; Howard, J. C.; Mark, E. H.; Datta Gupta, N. *Nucleic Acids Res.* **1979**, *6*, 3093.
(49) Pasternack, R. F.; Garrity, P.; Ehrlich, B.; Davis, C. B.; Gibbs, E. J.; Orloff, G.; Giartosio, A.; Turano, C. *Nucleic Acids Res.* **1986**, *14*, 5919.
(50) Pasternack, R. F.; Gibbs, E. J.; Villafranca, J. J. *Biochemistry* **1983**, *22*, 2406.
(51) Kelly, J. M.; Murphy, M. J.; McConnell, D. J.; OhUigin, C. *Nucleic Acids Res.* **1985**, *13*, 167.
(52) Lipscomb, L. A.; Zhou, F. X.; Presnell, S. R.; Woo, R. J.; Peek, M. E.; Plaskon, R. R.; Williams, L. D. *Biochemistry* **1996**, *35*, 2818.
(53) Pyle, A. M.; Long, E. C.; Barton, J. K. *J. Am. Chem. Soc.* **1989**, *111*, 4520.
(54) Pyle, A. M.; Rehmann, J. P.; Meshoyrer, R.; Kumar, C. V.; Turro, N. J.; Barton, J. K. *J. Am. Chem. Soc.* **1989**, *111*, 3051.
(55) Pyle, A. M.; Morii, T.; Barton, J. K. *J. Am. Chem. Soc.* **1990**, *112*, 9432.
(56) Sitlani, A.; Long, E. C.; Pyle, A. M.; Barton, J. K. *J. Am. Chem. Soc.* **1992**, *114*, 2303.
(57) Campisi, D.; Morii, T.; Barton, J. K. *Biochemistry* **1994**, *33*, 4130.
(58) Erkkila, K. E.; Barton, J. K. Manuscript in preparation.
(59) Sitlani, A.; Barton, J. K. *Biochemistry* **1994**, *33*, 12100.
(60) Chow, C. S.; Barton, J. K. *J. Am. Chem. Soc.* **1990**, *112*, 2839.
(61) Jenkins, Y.; Friedman, A. E.; Turro, N. J.; Barton, J. K. *Biochemistry* **1992**, *31*, 10809.
(62) Chow, C. S.; Barton, J. K. *Biochemistry* **1992**, *31*, 5423.
(63) Chow, C. S.; Behlen, L. S.; Uhlenbeck, O. C.; Barton, J. K. *Biochemistry* **1992**, *31*, 972.
(64) Lim, A. C.; Barton, J. K. *Biochemistry* **1993**, *32*, 11029.
(65) Chow, C. S.; Hartmann, K. M.; Rawlins, S. L.; Huber, P. W.; Barton, J. K. *Biochemistry* **1992**, *31*, 3534.
(66) Lim, A. C.; Barton, J. K. *Biochemistry* **1998**, *37*, 9138.
(67) Lim, A. C.; Barton, J. K. *Bioorg. Med. Chem.* **1997**, *5*, 1131.
(68) Sitlani, A.; Dupureur, C. M.; Barton, J. K. *J. Am. Chem. Soc.* **1993**, *115*, 12589.
(69) Jackson, B. A.; Barton, J. K. *J. Am. Chem. Soc.* **1997**, *119*, 12986.
(70) Jackson, B. A.; Alekseyev, V. Y.; Barton, J. K. *Biochemistry* **1999**, *38*, 4655.
(71) Krotz, A. H.; Kuo, L. Y.; Shields, T. P.; Barton, J. K. *J. Am. Chem. Soc.* **1993**, *115*, 3877.
(72) Krotz, A. H.; Kuo, L. Y.; Barton, J. K. *Inorg. Chem.* **1993**, *32*, 5963.
(73) Shields, T. P.; Barton, J. K. *Biochemistry* **1995**, *34*, 15037.
(74) Shields, T. P.; Barton, J. K. *Biochemistry* **1995**, *34*, 15049.
(75) Krotz, A. H.; Hudson, B. P.; Barton, J. K. *J. Am. Chem. Soc.* **1993**, *115*, 12577.
(76) Hudson, B. P.; Dupureur, C. M.; Barton, J. K. *J. Am. Chem. Soc.* **1995**, *117*, 9379.
(77) Sardesai, N. Y.; Barton, J. K. *J. Biol. Inorg. Chem.* **1997**, *2*, 762.
(78) Sardesai, N. Y.; Zimmermann, K.; Barton, J. K. *J. Am. Chem. Soc.* **1994**, *116*, 7502.
(79) Terbrueggen, R. H.; Barton, J. K. *Biochemistry* **1995**, *34*, 8227.
(80) Terbrueggen, R. H.; Johann, T. W.; Barton, J. K. *Inorg. Chem.* **1998**, *37*, 6874.
(81) Franklin, S. J.; Barton, J. K. *Biochemistry* **1998**, *37*, 16093.
(82) Odom, D. T.; Parker, C. S.; Barton, J. K. *Biochemistry* **1999**, *38*, 5155.
(83) Dervan, P. B. *Science* **1986**, *232*, 464.
(84) Pogozelski, W. K.; Tullius, T. D. *Chem. Rev.* **1998**, *98*, 1089.

(85) Hegg, E. L.; Burstyn, J. N. *Coord. Chem. Rev.* **1998**, *173*, 133.
(86) Fitzsimons, M. P.; Barton, J. K. *J. Am. Chem. Soc.* **1997**, *119*, 3379.
(87) Le Doan, T.; Perrouault, L.; Rougee, M.; Bensasson, R.; Helene, C. *In Photodynamic Therapy of Tumors and Other Diseases*; Jori, G., Perria, C., Eds.; Libreria Progetto: Padova, Italy, 1985; pp 56−58.
(88) Holmlin, R. E.; Dandliker, P. J.; Barton, J. K. *Angew. Chem.* **1997**, *109*, 2830; *Angew. Chem., Intl. Ed.* **1997**, *36*, 2714.
(89) Pratviel, G.; Bernadou, J.; Meunier, B. *Met. Ions Biol. Syst.* **1996**, *33*, 399.
(90) Vialas, C.; Pratviel, G.; Claparols, C.; Meunier, B. *J. Am. Chem. Soc.* **1998**, *120*, 11548.
(91) Johnston, D. H.; Cheng, C.-C.; Campbell, K. J.; Thorp, H. H. *Inorg. Chem.* **1994**, *33*, 6388.
(92) Napier, M. E.; Loomis, L. R.; Sistare, M. F.; Kim, J.; Eckhardt, A. E.; Thorp, H. H. *Bioconjugate Chem.* **1997**, *8*, 906.
(93) Carter, P. J.; Cheng, C.-C.; Goll, J. G.; Campbell, K. J.; Thorp, H. H. *J. Am. Chem. Soc.* **1998**, *120*, 632.
(94) Foote, C. S.; Shook, F. C.; Abakerli, R. B. *Methods Enzymol.* **1984**, *105*, 36.
(95) Armitage, B. *Chem. Rev.* **1998**, *98*, 1171.
(96) Mei, H. Y.; Barton, J. K. *Proc. Natl. Acad. Soc. U.S.A.* **1988**, *85*, 1339.
(97) Arkin, M. R.; Stemp, E. D. A.; Coates-Pulver, S.; Barton, J. K. *Chem. Biol.* **1997**, *4*, 389.
(98) Saito, I.; Takayama, M.; Sugiyama, H.; Nakatani, K.; Tsuchida, A.; Yamamoto, M. *J. Am. Chem. Soc.* **1995**, *117*, 6406.
(99) Prat, F.; Houk, K. N.; Foote, C. S. *J. Am. Chem. Soc.* **1998**, *120*, 845.
(100) Burrows, C. J.; Muller, J. G. *Chem. Rev.* **1998**, *98*, 1109.
(101) Stemp, E. D. A.; Arkin, M. R.; Barton, J. K. *J. Am. Chem. Soc.* **1997**, *119*, 3379.
(102) Hall, D. B.; Holmlin, R. E.; Barton, J. K. *Nature* **1996**, *382*, 731.
(103) Turro, C.; Evanhazav, A.; Bossmann, S. H.; Barton, J. K.; Turro, N. J. *Inorg. Chim. Acta* **1996**, *243*, 101.
(104) Hall, D. B.; Barton, J. K. *J. Am. Chem. Soc.* **1997**, *119*, 5045.
(105) Rajski, S. R.; Kumar, S.; Roberts, R. J.; Barton, J. K. *J. Am. Chem. Soc.* **1999**, *121*, 5615.
(106) Nunez, M. E.; Hall, D. B.; Barton, J. K. *Chem. Biol.* **1999**, *6*, 85.
(107) Dandliker, P. J.; Holmlin, R. E. Barton, J. K. *Science* **1997,** *275*, 1465.
(108) Dandliker, P. J.; Nunez, M. E.; Barton, J. K. *Biochemistry* **1998**, *37*, 6491.

CR9804341